Materials Advances

ROYAL SOCIETY OF CHEMISTRY

REVIEW

View Article Online
View Journal | View Issue

Cite this: *Mater. Adv.*, 2021, 2, 6136

Indole fused heterocycles as sensitizers in dye-sensitized solar cells: an overview

P. R. Nitha,[ab] Suraj Soman *[ab] and Jubi John *[ab]

Received 8th June 2021,
Accepted 19th August 2021

DOI: 10.1039/d1ma00499a

rsc.li/materials-advances

The past three decades have witnessed extensive research in developing a range of non-metallic organic dyes for dye sensitized solar cells (DSSCs). Dyes occupy a prominent position among components in DSSCs, and organic dyes have emerged as the most promising candidate for DSSCs due to their performance, ease of synthesis, stability, tunability, low cost and eco-friendly characteristics. In addition to this, so far, the best and highest performing DSSCs reported in the literature use metal-free organic dyes. Organic dyes also provide flexibility to be used along with alternate new generation cobalt and copper electrolytes. Among various organic dyes, heterocycles, mainly N- and S-containing, have found immense applications as sensitizers. Indole fused heterocycles were used by different research groups in their dye designs, mainly as a donor and π-spacer. The planarity of these electron-rich fused indole systems is advantageous as it helps to initiate a more prominent ICT transition in dye molecules. In addition, the possibility for selective functionalization of N-atoms with long or branched alkyl chains prevents the aggregation of the sensitizer, increasing the solubility and is effective in custom design dyes which are in turn capable of preventing back electron transfer (recombination). Fused indole moieties utilized in the design of sensitizers are stable and offer easy synthesis. In the present review, we examine different indole fused heterocycles as building blocks for sensitizers used in DSSCs.

Introduction

Fossil fuel-based resources have been primarily satisfying the energy demands of humankind for more than a century. The ever-increasing energy demands that are fuelled by the growing

[a] *Chemical Sciences and Technology Division, CSIR-National Institute for Interdisciplinary Science and Technology (CSIR-NIIST), Thiruvananthapuram 695019, India. E-mail: suraj@niist.res.in, jubijohn@niist.res.in*
[b] *Academy of Scientific and Innovative Research (AcSIR), Ghaziabad-201002, India*

P. R. Nitha

P. R. Nitha was born in 1992 in Thrissur, Kerala. She obtained her BSc Degree from K. K. T. M. College (University of Calicut), Kodungallur in 2012 and her MSc Degree from Cochin university of Science and Technology in 2014. She is currently pursuing her doctoral research on utilization of indole fused heterocycles for DSSC applications, under the combined supervision of Dr Jubi John and Dr Suraj Soman at the National Institute for Interdisciplinary Science and Technology (CSIR-NIIST), Thiruvananthapuram.

Suraj Soman

Dr Suraj Soman obtained his PhD in molecular photocatalysis from Dublin City University (Ireland) under the supervision of Prof. Han Vos and Prof. Mary Pryce followed by postdoctoral tenure at Michigan State University (USA) with Prof. Thomas W. Hamann. Dr Suraj Soman joined CSIR-NIIST (India) in 2014 and is currently working as a Scientist at CSIR-NIIST. His prime research focus involves all aspects of Dye Sensitized Solar Cells (DSSCs) spanning from materials to devices to detailed dynamic measurements. His interdisciplinary research group also focus in module/prototype development through academia-industry collaborations in a way to exploit DSSC technology for indoor photovoltaics & BIPV applications.

human population have contributed to environmental issues with the depletion of conventional resources, necessitating the need for research into developing efficient methods to harness alternative energy sources.[1] Solar energy is considered one of the most promising alternatives that could sustainably provide inexhaustible energy.[2] The stepping stone for photovoltaic technology was laid with the demonstration of the first silicon-based solar cells by Bell laboratories, which exhibited an efficiency of ~6%. Since then, the technology has witnessed many advancements in introducing thin films in the late 1970's and finally reaching up to the third-generation solar cells.[3] The third-generation photovoltaics consist of dye-sensitized solar cells, organic solar cells, quantum dot solar cells and perovskite solar cells.[4] Though their efficiencies are still lagging behind the conventional silicon-based devices, the lower fabrication cost of these devices along with lesser environmental impact are promising factors that urge the scientific community to carry out research and technological advancements in third-generation photovoltaics.[5]

Dye sensitized solar cell research got momentum in 1991 with the pioneering work carried out by Brian O'Regan and Michael Gratzel, where they used Ru metal complex sensitized nanocrystalline TiO_2 film, generating a power conversion efficiency of 7%.[6] DSSCs have many attractive features, including lower fabrication cost and short payback time with minimum environmental hazards.[7] In addition, they can be designed for both outdoor as well as indoor light harvesting.[8] DSSC consists of three major components, photoelectrode, electrolyte and a counter electrode. The dye sensitized mesoporous semiconductor layer coated on a conductive glass/plastic substrate collectively acts as the photoanode. The electrolyte is responsible for both regeneration of the dye as well as charge transport to the counter electrode. Liquid electrolytes which consist of redox mediators in organic solvents are typically used in DSSCs. To address the leakage and device lifetime issues originating from the usage of liquid electrolytes, efforts are being made to explore quasi-solid electrolytes and solid conductors. The counter electrode is composed of transparent conductive oxides (ITO/FTO) coated with catalysts like platinum for fast electron transfer reactions. The mechanism of current generation with DSSCs starts with the absorption of light by the dye sensitizers that are adsorbed on the semiconductor surface. These photo-excited electrons are then injected into the conduction band of the semiconductor, which diffuses through the conductive substrate and finally reaches the counter electrode. The oxidized dye molecules are subsequently regenerated by the redox mediators present in the electrolyte, which are then reduced at the counter electrode. This cycles continues generating current without net chemical change in the system (Scheme 1).[9]

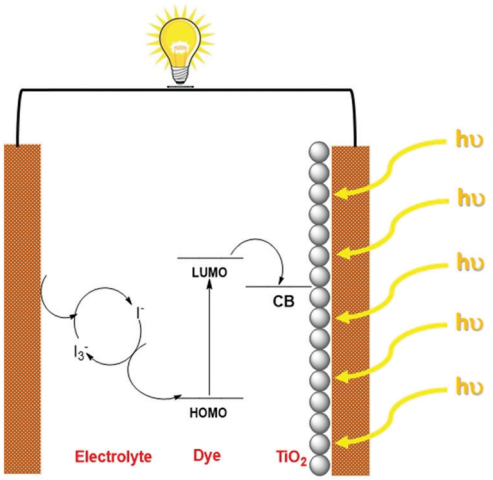

Scheme 1 Operating principle of DSSCs.

Unlike conventional PV devices, DSSCs excel with the advantage that different components are carrying out light absorption, charge generation, and charge transport. This opens up the broader possibility of achieving higher photovoltaic performance by selectively optimizing each component used in the device. The sensitizer represents the core unit in DSSCs, responsible for light absorption and electron injection into the semiconductor layer. An ideal sensitizer is supposed to display panchromatic absorption with a higher molar extinction coefficient. The optimum redox potential of the dye energy levels (HOMO–LUMO) is necessary to achieve efficient electron injection into the semiconductor conduction band and to realize effective regeneration of the dye ground state by the redox electrolyte. The sensitizer should also possess features such as suitable binding groups (–COOH, $-PO_3H_2$) to anchor onto the semiconductor surface and also needs to be engineered in such a way to minimize aggregation on the semiconductor. The prevention of dye aggregation is highly desirable to reduce recombination losses and increase the open circuit potential of the devices, which can also contribute to the stability of the device as a whole.[10]

Ruthenium-based sensitizers dominated the first two decades in DSSC research since their inception in the early nineties due to their broad absorption and higher power conversion efficiencies

Jubi John

Dr Jubi John obtained his PhD in synthetic organic chemistry from CSIR-NIIST under the supervision of Dr K. V. Radhakrishnan. Soon after he joined as a CEA-Eurotalents postdoctoral fellow with Dr Eric Doris at CEA Saclay, France. In 2011, he joined as an Alexander von Humboldt fellow with Prof. Henning Hopf at TU Braunschweig, Germany and from 2013, with Prof. Wim Dehaen at the KU Leuven, Belgium. He then joined CSIR-NIIST in 2015 and is presently working as a senior scientist at the same institute. His research interests include development of novel synthetic methodologies, new antiviral drug candidates and dyes for material applications.

and reached up to a PCE of 11.5% using a conventional iodide/triiodide electrolyte.[11] Though these sensitizers appear to be feasible for practical applications, with progressing research, a lower molar extinction coefficient of metal complexes along with the scarcity of Ru have slowly paved the way for the advent of metal-free sensitizers. Additionally, the introduction of alternate cobalt and copper electrolyte further encouraged the scientific community to expand the research on organic dyes, which are most suitable with alternate electrolytes. The introduction of metal-free sensitizers has also opened up an arsenal of strategies to develop more efficient devices at a lower cost and in an eco-friendly manner.[12] Metal-free sensitizers generally display high molar extinction coefficients, but the narrow absorption of many sensitizers results in serious concern over light harvesting. The emergence of a co-sensitization strategy helped to alleviate this limitation by realizing panchromatic absorption through the sensitization of a combination of different dyes having complementary absorption.[13] This also reduced the possibility for dye aggregation. The strongest side of organic sensitizers involves the flexibility in tuning the chemical structure with the help of the well-established synthetic strategies.[14] According to the recent reports, the PCE of DSSCs based on single metal free organic sensitizers has reached 13.6% using a cobalt electrolyte, 11.7 for solid state DSSCs and 32% for indoor light harvesting. The co-sensitization strategy could realize 14.3% PCE using a cobalt based electrolyte.[15]

Molecular engineering of dyes deals with designing systems with potential light-harvesting ability over the entire visible region with proper energetics that realizes electron transfer from the excited state of the dye to the metal oxide upon light absorption. The most widely employed molecular architecture is the donor–π spacer–acceptor (D–π–A) strategy.[16] Anchoring groups are supposed to be bifunctional, serving the purposes of adsorption as well as electron acceptance. Although many new anchoring groups have emerged, a cyanoacrylate group is generally found to outperform others because of its agreement with the two functions mentioned above. The strong electron withdrawing nature of the cyanoacrylate moiety facilitates the broadening of the absorption spectra of molecules and the strong adsorption capability to the semiconductor surface increases the injection ability and device lifetime. A wide variety of choices are present for both donor and π-spacer moieties. The derivatives of arylamine, carbazole, coumarins and phenothiazine are some of the popular donor groups of continued interest used in DSSCs.[17] The π-linkers are also of paramount importance in tuning the communication between donor and acceptor units, thereby increasing the light-harvesting ability of the dyes. Though thiophene, furan, benzene and oligothiophenes have been used extensively as π-spacers in dyes, fused ring planar systems with strategies to prevent π–π aggregation have not been explored to the full extent.[18] Apart from modulating each building block of a sensitizer, considerable effort was also laid in engineering new dye design strategies, which resulted in the introduction of architectures like D–A–π–A, D–D–π–A, A–π–D–π–A and D–π–A–A.[19]

The present review attempts to consolidate and analyse dye sensitizers which utilize fused indole units as components in sensitizers used in DSSCs. These indole-fused heterocycles are found to exhibit more electron-donating ability than those with indole in conjugation with expanded π-systems.[20] Another advantage of the fused indole systems is the better planarity they possess, inducing better donor–acceptor interaction leading to improved PV performance. The possibility of functionalization of the N-atom with long or branched alkyl chains is another advantage of indole-based heterocyclic systems that increase the solubility and prevent aggregation of the sensitizer. The majority of fused indoles were used as a donor moiety in the sensitizers, and very few units were used as π-spacers. The indole fused systems explored as building blocks in DSSC sensitizers include indoloquinoxaline (IQ), indolocarbazole, indoloindole, benzothienoindole, indenoindole, triazatruxene, thienoindole, tetraindole, dithienopyrroloindole, fluorenylindolenine, and indole–imidazole. The exploration of these systems as donor and π-spacers are investigated fitting in different molecular architectures. This will help the scientific community further re-engineer these heterocycles with excellent optoelectronic properties in line with the requirements of the photovoltaic applications.

I. Indoloquinoxaline based sensitizers for DSSCs

Indolo[2,3-*b*]quinoxaline (IQ), a built-in donor–acceptor chromophore, consists of an electron-rich indole moiety fused with an electron-deficient quinoxaline unit. The condensation of isatin with *o*-phenylenediamine can efficiently synthesize these planar heteroarenes.[21] By appropriately functionalizing the indole and quinoxaline motifs with electron-donating or electron-withdrawing groups, the electronic properties of this chromophore can be custom-tuned in line with the applications. It has been documented that the donating ability of the indole motif and the donor–acceptor interaction with the quinoxaline unit is enhanced by functionalizing the indole core with electron-donating groups.[22]

The first utilization of this scaffold as a building block in DSSCs was carried out by Venkateswararao *et al.*[23] They constructed dyes **2–6**, which are having IQ as an electron donor and cyanoacrylic acid as an anchoring unit (Fig. 1). The sensitizers differed in the π-spacer employed, which were either phenyl or thiophene fragments. Dye **1**, which lacks any π-spacer, delivered the least efficiency of 0.86%. Among the remaining sensitizers, **6** showed a red shifted and distinct ICT band implying more effective conjugation. Two dye baths were used to fabricate devices, one with DCM and the other with a combination of CH_3CN/*tert*-butanol/DMSO (3.5/3.5/3, v/v). All the sensitizers exhibited better efficiencies in the latter case. The changes in PCE were mainly caused by significant changes in the photocurrent generated. Though ICT was more prominent in the case of **6**, a relatively high degree of planarity might have caused aggregation of the dyes leading to decreased light harvesting. Dye **2** with simple thiophene as the π-spacer outperformed other dyes with PCE of 3.45% with J_{sc} of 9.29 mA cm^{-2} and V_{oc} of 579 mV.

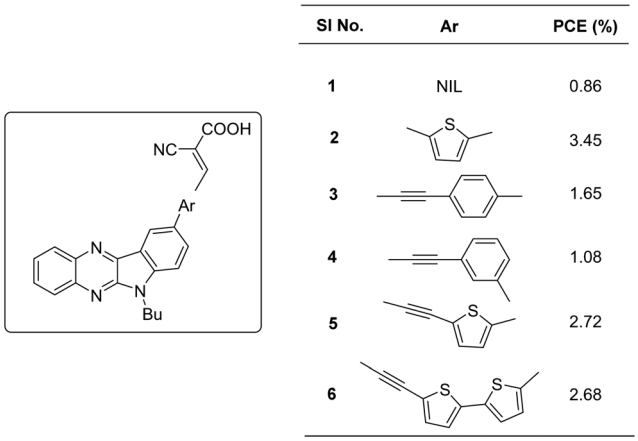

Fig. 1 Photosensitizers **1–6** based on an indolo[2,3-*b*]quinoxaline core.

Other dyes showcased PCE in the order **6** > **5** > **3** > **4** (Table 1). The introduction of acetylene was not found to be beneficial for transmitting charges in the current design.

Later, Qian *et al.* developed three D–π–A dyes having indolo[2,3-*b*]quinoxaline and cyanoacrylic acid as donor and acceptor groups, respectively.[24] Sensitizers **7**, **8**, and **9** differ in the selection of conjugated spacers, which were oligothiophene, thienylcarbazole, and furylcarbazole, respectively (Fig. 2). The dyes exhibited efficiencies in the order **7** > **9** > **8** (Table 1). The maximum efficiency of 7.62% was delivered by **7**, mainly contributed by the significantly larger short circuit current density (J_{sc} = 16 mA cm^{-2}) of this dye. The electron-rich, oligothiophene π-bridge makes the absorption spectra of **7** more red-shifted with an absorption maximum at 480 nm for the ICT band followed by **8** and **9**. The IPCE performance of the devices is following the absorption behaviour of the dyes. While **7** shows broad absorption from 400 to 770 nm, in the case of **8** and **9**, the absorption furnishes onset at 700 and 690 nm, respectively illustrating the trend in the dyes' J_{sc} and light-harvesting ability. Though lower current density was delivered by **9**, the higher open circuit potential (V_{oc} = 742 mV) helped **9** outperform **8**.

Table 1 Photovoltaic parameters of indoloquinoxaline based DSSCs

Sensitizer	J_{sc} (mA cm^{-2})	V_{oc} (mV)	FF	PCE (%)	Electrolyte	Coadsorbent (concentration)	Ref.
1	2.66	500	0.64	0.86	I^-/I_3^-	—	23
2	9.29	579	0.64	3.45	I^-/I_3^-	—	23
3	4.43	543	0.68	1.65	I^-/I_3^-	—	23
4	2.73	593	0.67	1.08	I^-/I_3^-	—	23
5	7.38	568	0.65	2.72	I^-/I_3^-	—	23
6	7.77	562	0.62	2.68	I^-/I_3^-	—	23
7	16.0	708	0.67	7.62	I^-/I_3^-	—	24
8	14.8	701	0.63	6.48	I^-/I_3^-	—	24
9	14.1	742	0.67	7.03	I^-/I_3^-	—	24
10	8.9	676	0.68	4.10	I^-/I_3^-	—	25
11	14.0	705	0.69	6.82	I^-/I_3^-	—	25
12	15.3	757	0.71	8.28	I^-/I_3^-	—	25
13	14.2	745	0.71	7.56	I^-/I_3^-	—	25
14	11.9	797	0.64	6.05	I^-/I_3^-	—	26
15	12.9	817	0.67	7.09	I^-/I_3^-	—	26
16	9.03	707	0.68	4.35	I^-/I_3^-	—	26
17	9.71	724	0.68	4.81	I^-/I_3^-	—	26
18	5.56	653	0.72	2.65	I^-/I_3^-	CDCA (10 mM)	27
19	5.68	622	0.73	2.72	I^-/I_3^-	CDCA (10 mM)	27
20	5.99	618	0.69	2.61	I^-/I_3^-	CDCA (10 mM)	27
21	19.0	649	0.61	7.46	I^-/I_3^-	CDCA (20 mM)	27
19/21	19.37	654	0.63	7.94	I^-/I_3^-	CDCA (20 mM)	27
22	4.73	637	0.73	2.21	I^-/I_3^-	CDCA (10 mM)	28
23	5.08	676	0.74	2.56	I^-/I_3^-	CDCA (10 mM)	28
22/21	17.79	683	0.67	8.16	I^-/I_3^-	CDCA (20 mM)	28
23/21	18.24	688	0.69	8.67	I^-/I_3^-	CDCA (20 mM)	28
24	11.10	676	0.70	5.27	I^-/I_3^-	CDCA (10 mM)	29
25	11.29	657	0.69	5.10	I^-/I_3^-	CDCA (10 mM)	29
26	11.84	638	0.65	4.92	I^-/I_3^-	CDCA (10 mM)	29

Soon after, the authors used the same scaffold to realize D–D–π–A and D–π–A systems.[25] In D–D–π–A design, indoloquinoxaline was used as the primary donor and phenothiazine was used as an auxiliary donor, cyanoacrylic acid as an acceptor and thiophene/furan as a π-bridge to afford **12** and **13**, respectively (Fig. 3). These dyes were then compared with **10** and **11**, which were D–π–A dyes based on indoloquinoxaline and phenothiazine, respectively, as donors. Among the dyes, **12** having D–D–π–A design was found to outperform the rest. Sensitizer **12** excelled with an efficiency of 8.28% followed by **13** with 7.56%. Compared to furan, the electron richness of thiophene was aiding good ICT transitions reducing the HOMO–LUMO gap for **12**, which resulted in more red-shifted and enhanced absorption spectra for **12** compared to that of **13** with furan as a π-spacer. The IPCE spectra of the dyes show a similar trend, with **12** giving over 60% IPCE value from 359 to 600 nm with maximum absorption of 86% at 490 nm. This illustrates the reason for the highest light-harvesting ability and J_{sc} (15.3 mA cm^{-2}) for **12**. The V_{oc} values obtained are in the order **12** > **13** > **11** > **10** (Table 1).

Later in 2017, the authors utilized indoloquinoxaline as an acceptor in a $(D)_2$–A–π–A dye design in which two triphenylamine groups were used as two branches of the primary donor unit. The dyes **14–17** differed in the π-bridges (furan and thiophene) and acceptor groups (cyanoacrylic acid and 2-(1,1-dicyanomethylene)rhodanine or DCRD) (Fig. 4).[26] These dyes exhibited efficiencies in the range of 4.55% to 7.09%. Dyes **14** and **15**, which had cyanoacrylic acid as the acceptor group, outperformed the corresponding dyes having DCRD as the acceptor unit. Though the absorption spectra of **16** and **17** were much red-shifted compared to **14** and **15**, higher dye loading of the latter resulted in larger J_{sc} values. This is also apparent from the IPCE spectra. Though the spectra of **14** and **15** are blue-shifted with 30 and 20 nm differences respectively with respect to **17**, the increase in J_{sc} value contributed to a better PV performance. Dye **15** could deliver over 60% IPCE value from 400 to 600 nm with a maximum of 83% at 450 nm, resulting in a J_{sc} value of 12.9 mA cm^{-2} (Table 1). While comparing the π-spacers, furan substituted sensitizers **15** and **17** were found to deliver better efficiencies than their thiophene substituted counterparts. While **15** delivered a PCE of 7.09% with the highest J_{sc} and V_{oc} values, **14** slightly lagged with a power conversion efficiency of 6.05%. DCRD substituted dyes **16** and **17** showcased relatively poor performances with a PCE of 4.55% and 4.81%, respectively.

Later, Su and co-workers introduced sensitizers **18–20** based on new molecular architecture, D–D|A–π–A (Fig. 5).[27] Here, D|A

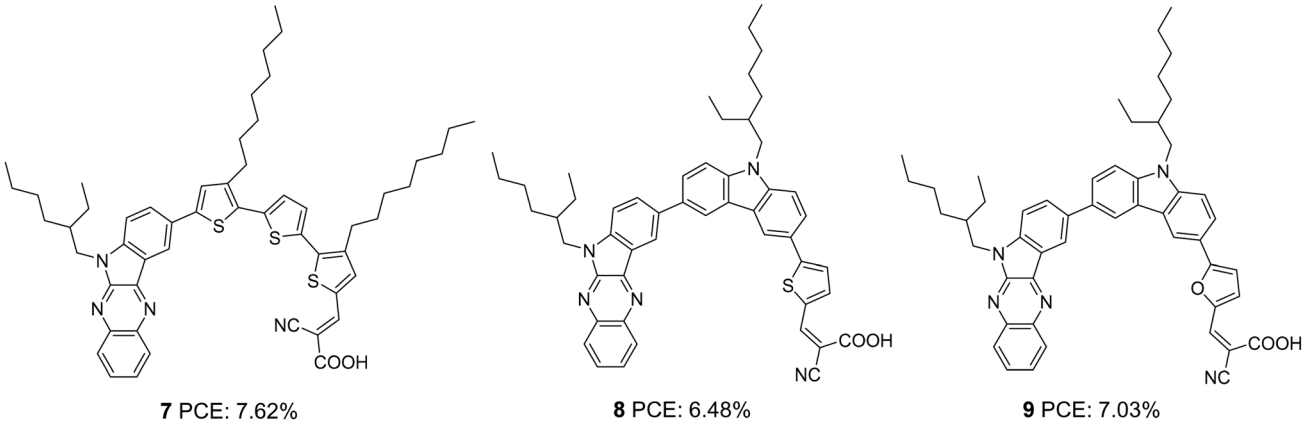

Fig. 2 Photosensitizers **7–9** based on an indolo[2,3-*b*]quinoxaline core.

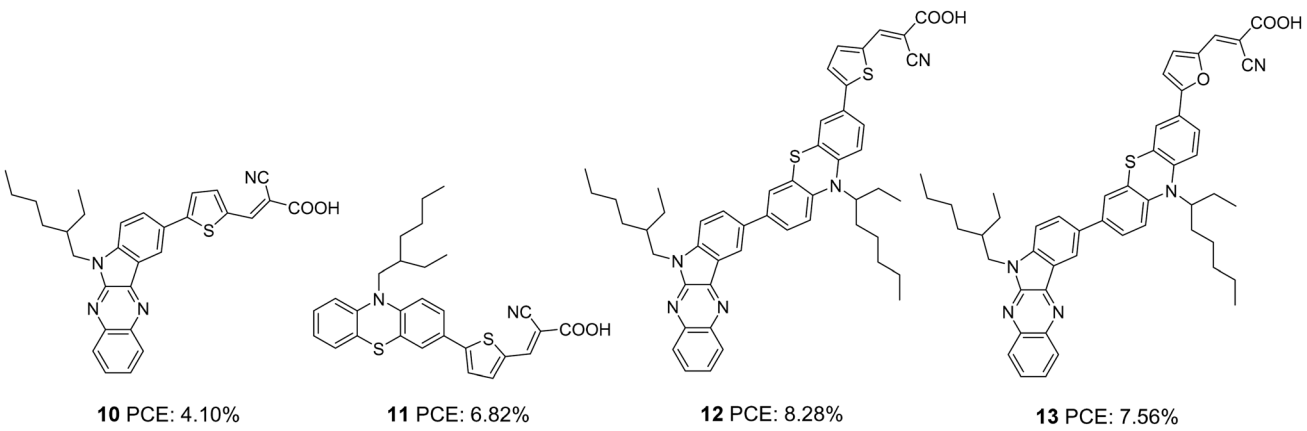

Fig. 3 Photosensitizers **10–13** based on indolo[2,3-*b*]quinoxaline and phenothiazine cores.

represents the fused donor–acceptor unit, indolo[2,3-*b*]quinoxaline. The effect of additional donors was investigated systematically by introducing triphenylamine, carbazole and phenothiazine donors to the indole unit. More significant dye loading in devices based on **18** resulted in effective monolayer formation on the TiO_2 surface, thereby preventing recombination effectively. This contributed to the highest open-circuit potential for devices fabricated using **18**. When it comes to photocurrent, the hexyl chains incorporated on the end donors of **19** and **20** helped decrease aggregations, contributing to improved J_{sc}. Maximum efficiency was delivered by **19** (2.72%), followed by **18** (2.65%) and **20** (2.61%). Later, these new generation D–D/A–π–A organic dyes were used successfully as co-sensitizers to improve the PCE of conventional Ru dye (**21**). The device fabricated with **21** alone showed an efficiency of 7.46%. Co-sensitization of **18–20** improved the efficiency in all three cases with a maximum of 7.94%, when **19** was employed as a co-sensitizer with **21** (Table 1). An increment in open-circuit potential was observed with the co-sensitization approach, which could be attributed to the improved surface coverage of TiO_2, resulting in retardation of aggregation and recombination. When it comes to photocurrent, only the device with **19** as a co-sensitizer showed an increment in current density from 19.00 mA cm^{-2} to 19.37 mA cm^{-2}. More significant dye loading in the remaining cases might have resulted in competitive absorption at the overlapping regions between the Ru dye and organic co-sensitizer.

Later, Su *et al.* introduced a di-branched di-anchoring approach to the previous molecular architecture to develop D–D|A–$(\pi\text{–A})_2$ dyes **22** and **23**, which differed in additional donors between triphenylamine and carbazole, respectively (Fig. 6).[28] The performances were also compared with devices based on **19**. The dianchoring approach was found to help form adequate surface coverage, which is also evident from the higher dye loading present in these dyes. This could cause an increment in V_{oc} of dianchored dyes compared to **19** due to minimal recombination. Among the dianchored dyes, **23** with hexyl chain incorporated carbazole as the secondary donor exhibited the highest V_{oc}. Dye **19** excelled when photocurrent is taken into account, which even contributed to higher PCE compared to the rest. The downfall in light-harvesting efficiency of **22–23** was brought about by the increased dihedral angle and strain induced by the di-anchoring branches. A more prominent donating ability of carbazole caused a slightly higher increment in J_{sc} of **23** compared to **22**. Co-sensitization of these

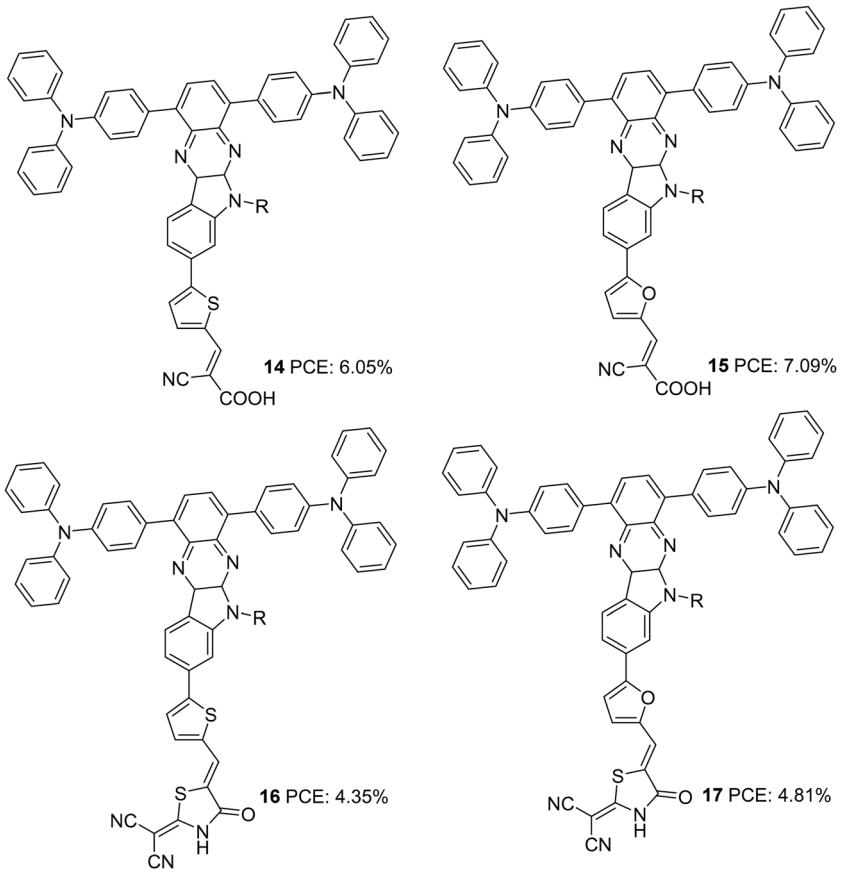

Fig. 4 Photosensitizers **14–17** with an indolo[2,3-*b*]quinoxaline core.

dyes with **21** could enhance the efficiency with the highest PCE of 8.67% for **23**, followed by **13** (8.16%) and **19** (7.50%). While the considerably improved V_{oc} contributed the increment in device performance of co-sensitized **22-23**, a slight increment in current density for **19** caused a corresponding increment in PCE.

In the subsequent work, the π-spacer in **18–20** was changed to thiophene from benzene, and the performance of the sensitizers (**24–26**) was evaluated under full sun illumination (Fig. 7).[29] The dyes exhibited efficiencies in the range 4.92–5.27%, which was higher than previously reported sensitizers having phenyl as a spacer. Dye **24**, having triphenylamine as a donor, displayed the maximum PCE of 5.27% with a V_{oc} of 0.67 V and FF of 70.1 with improved J_{sc} of 11.10 mA cm^{-2} (Table 1). Higher dye loading seems to be responsible for improving FF and open-circuit potential for the triphenylamine donor dye **24**. Though the highest photocurrent was observed for **26** due to its increased light-harvesting ability, comparatively lower values obtained for the rest of the parameters contributed towards inferior PCE of 4.92% for **26.** Co-sensitization of **21** with these dyes also resulted in improved V_{oc} and FF. In addition, the competition for light absorption resulted in a considerable reduction of photocurrent, leading to net poor performance for the co-sensitized device compared to the individual dyes.

From Table 1, it is clear that indoloquinoxaline is a potential scaffold for dye sensitizers in DSSCs. The highest efficiency achieved so far using IQ based sensitizer is 8.2%, where the IQ unit and π-spacer (thiophene) is attached to either end of the auxiliary donor (phenothiazine) with cyanoacrylic acid as the acceptor unit. In the same architecture itself, optimum tuning of auxiliary donors and π-spacers along with the alkyl groups could render sensitizers capable of delivering more than 10% PCE. From the reported sensitizers using IQ, it is impossible to generalize suitable π-spacers for the system that could change depending on the donor attached to it and the IQ position (indole/quinoxaline end) to which it is attached. Many studies were not carried out in this direction of anchoring units, opening up further possibilities towards efficient IQ-based devices.

II. Indolocarbazole based sensitizers for DSSCs

Indolocarbazole, especially indolo[3,2-*b*]carbazole isomer, is a linear pentacene with two N-atoms with the possibility of introducing alkyl chains of any length requirement either to improve solubility or to prevent back electron transfer. When compared to carbazole, indolocarbazole possesses better energetics, improved electron-donating capabilities and superior absorption profiles. These characteristics find indolocarbazoles

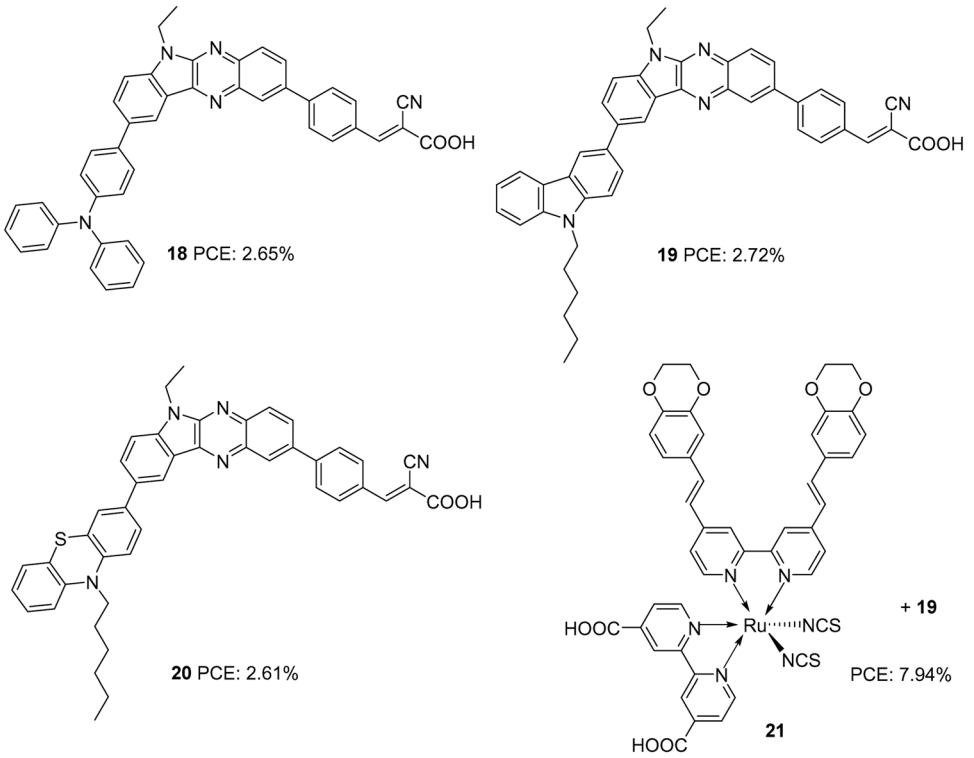

Fig. 5 Photosensitizers with an indolo[2,3-*b*]quinoxaline moiety and Ru-complex.

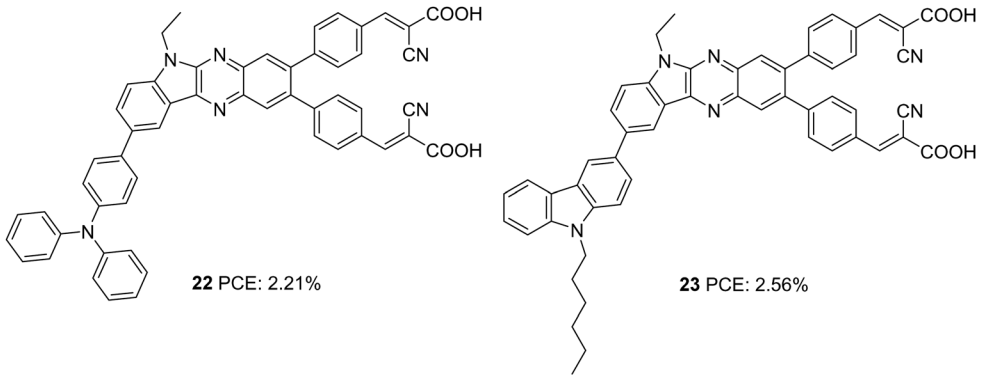

Fig. 6 Photosensitizers **22–23** with an indolo[2,3-*b*]quinoxaline moiety.

a unique position among various applications involving organic thin-film transistors, organic light-emitting diodes and photovoltaics.[30] Indolocarbazoles can be prepared either by Fischer indole synthesis of 1,4-bis(2-phenylhydrazono)cyclohexane or by a Cadogen reaction of appropriate nitroarenes.[31]

Indolocarbazole was first used as a donor in DSSCs by Zang *et al.* (Fig. 8).[32] They synthesized dyes **27** and **28**, which differ in the number of thiophene groups incorporated as the π-linker. While a red shift in the absorption profile was observed for **28** when adsorbed on TiO_2, higher electron injection efficiency was obtained for **27** sensitized devices. The trade-off between the two factors renders **28** with slightly higher J_{sc} compared to that of **27**. The difference in efficiencies of the two dyes were also brought about by the fill factor. While **27** possesses a FF of 0.67, the larger molecular size of **28** resulted in a FF of 0.62 (Table 2). This resulted in a higher PCE of 7.3% for **27** and 6.7% for **28**.

Cai *et al.* designed four dyes based on 5,7-dihexyl-6,12-diphenyl-5,7-dihydroindolo[2,3-*b*]carbazole (DDC) with benzothiadiazole (or thiophene) and thieno[3,2-*b*]thiophene (TT) (or thiophene) as the π-spacer and 2-cyanoacrylic acid as an acceptor (Fig. 9).[33] Along with the high electron-donating ability, the fused carbazole systems also contribute towards improved π-conjugation, which will be advantageous in promoting the ICT and the photostability of the system. The two phenyl rings integrated on the donor DDC unit, and the alkyl groups on the nitrogen atom effectively reduced the aggregation

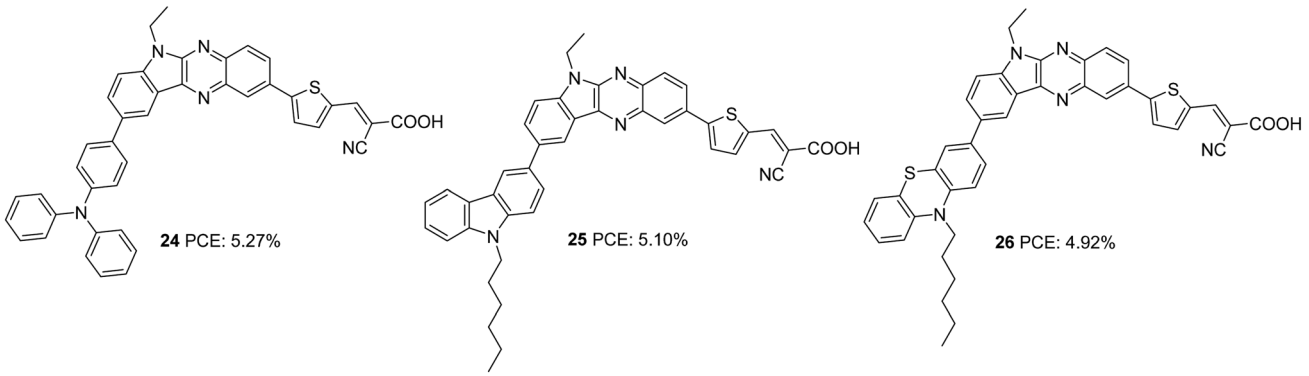

Fig. 7 Photosensitizers **24–26** with an indolo[2,3-*b*]quinoxaline moiety.

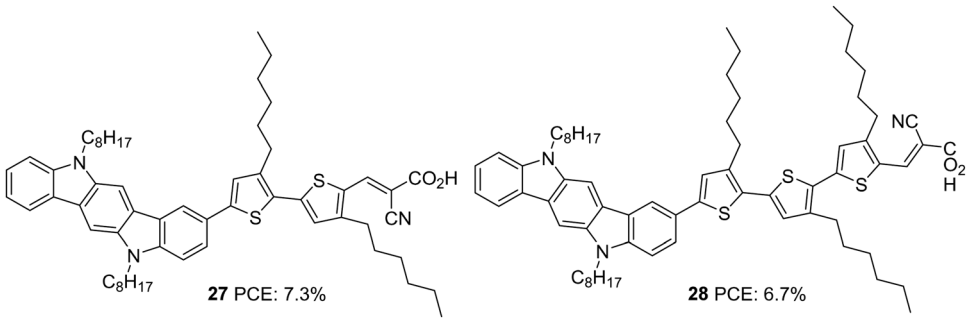

Fig. 8 Photosensitizers **27–28** with an indolocarbazole moiety.

and improved the lifetime for devices fabricated with these dyes. The devices were also subjected to comparison with carbazole based D–π–A sensitizer **33**. The molar extinction coefficients of both ICT and π–π transition bands display significant enhancement in **29–32** compared to **33** indicating the improved light-harvesting ability of the new fused conjugated donor. Except for **31**, the J_{sc} value for all other dyes was higher than **33**. This is apparent from the IPCE spectra, where the performance follows the order **32** > **29** > **30** > **33** > **31**, which is consistent with the dye loading present in the fabricated devices. Though the V_{oc} value of **32** (674 mV) was not very high compared to **31** (768 mV), **32** exhibited the highest efficiency of 6.4% among these sensitizers with a J_{sc} of 13.96 mA cm^{-2} and FF of 0.68 (Table 2). The photostability evaluation of the dyes by adopting the methods of Katoh and co-workers revealed that the new donor is effective in stabilizing the cation formed after irradiation of light compared to the carbazole based dye. The benzothiadiazole containing dyes possess more stability which is consistent with the previous reports.[34] The results also paved the way to the observation that TT was also beneficial for contributing towards photostability. Compound **32**, having both BTD and TT as a π-spacer, exhibited maximum photostability, while **29** was least stable among the indolocarbazole based dyes. All the dyes were also found to be thermally stable.

The same group further attempted to introduce a bridge with extended conjugation to widen the absorption spectra of the indolocarbazole dyes (Fig. 10).[35] Among the dyes, **36**, which contains benzothiadiazole as an auxiliary acceptor along with alkylated thiophenes flanked on both sides, showed maximum red-shifted spectra followed by **35** having alkyl-substituted benzothiadiazole as an auxiliary acceptor and **34** with simple D–π–A architecture having ter-thiophene as a spacer with a difference of 78 and 50 nm, respectively, compared to **36**. The device efficiency was tested under two conditions. In one case, the TiO_2 films were made of 3 μm thickness with 13 nm sized nanoparticles (TSP) and scattering layer of 4 μm thickness, and in the second case, the TiO_2 films were made of 3 μm thickness with 13 nm sized nanoparticles (TSP) and scattering layer of 8 μm thickness. Though higher dye loading is possible in the second case, a thick scattering layer can cause chances of recombination. This resulted in a trend of increase in current density and decrease in V_{oc} for all the dyes fabricated with an 8 μm scattering layer when compared to those of 3 μm thickness. A trade-off between these two factors leads to higher PCE with a thicker scattering layer for all the dyes. In the first condition, the highest IPCE value was obtained for **36** with an absorption maximum of 81.2% at 460 nm followed by **35** (77.2% at 500 nm) and **34** (69.9% at 520 nm). A more comprehensive absorption profile for **36** contributed towards the highest J_{sc} value of 14.91 mA cm^{-2}. The least J_{sc} value of 10.40 mA cm^{-2} was obtained for **34** due to the narrow IPCE spectra resulting from a lower absorption profile (Table 2). When devices were fabricated using an 8 μm scattering layer, dye **35** showed improved IPCE profile and J_{sc} value, while dye **36** resulted in lower molar extinction coefficients, low dye loading amount, and low electron injection yield. The trend in V_{oc} was the same in both the

Table 2 Photovoltaic parameters of indolocarbazole based DSSCs

Sensitizer	J_{sc} (mA cm^{-2})	V_{oc} (mV)	FF	PCE (%)	Electrolyte	Coadsorbent (concentration)	Ref.
27	15.4	710	0.67	7.3	I^-/I_3^-	—	32
28	15.5	700	0.62	6.7	I^-/I_3^-	—	32
29	11.95	768	0.66	6.09	I^-/I_3^-	—	33
30	11.57	707	0.68	5.55	I^-/I_3^-	—	33
31	9.40	644	0.68	4.11	I^-/I_3^-	—	33
32	13.96	674	0.68	6.40	I^-/I_3^-	—	33
33	10.28	713	0.67	4.90	I^-/I_3^-	—	33
34[a]	10.40	747	0.70	5.43	I^-/I_3^-	—	35
34[b]	12.92	710	0.66	6.01	I^-/I_3^-	—	35
35[a]	13.44	752	0.65	6.53	I^-/I_3^-	—	35
35[b]	16.41	706	0.64	7.49	I^-/I_3^-	—	35
36[a]	14.91	651	0.67	6.48	I^-/I_3^-	—	35
36[b]	15.88	620	0.68	6.64	I^-/I_3^-	—	35
37	12.6	729	0.68	6.25	I^-/I_3^-	—	36
38	15.2	745	0.71	8.09	I^-/I_3^-	—	36
39	13.9	738	0.68	6.98	I^-/I_3^-	—	36
40	14.1	757	0.71	7.58	I^-/I_3^-	—	36
41	5.69	750	0.72	3.11	I^-/I_3^-	CDCA (1 mM)	37
42	5.09	750	0.74	2.83	I^-/I_3^-	—	37
43	3.89	610	0.69	1.65	I^-/I_3^-	—	37
44	10.16	710	0.71	5.12	I^-/I_3^-	—	38
45	12.85	720	0.69	6.34	I^-/I_3^-	—	38
44/45	13.38	740	0.71	7.03	I^-/I_3^-	—	38
46	12.45	690	0.70	6.02	I^-/I_3^-	—	39
47	10.73	731	0.74	5.78	I^-/I_3^-	—	40
48	9.81	680	0.78	5.23	I^-/I_3^-	—	40
49	10.95	754	0.72	5.97	I^-/I_3^-	—	40
50	7.05	690	0.53	2.56	I^-/I_3^-	—	41
51	9.78	660	0.57	3.68	I^-/I_3^-	—	41
52	4.04	620	0.64	1.59	I^-/I_3^-	—	41
53	7.57	640	0.53	2.5	I^-/I_3^-	—	41
54	12.16	560	0.69	4.68	I^-/I_3^-	CDCA (10 mM)	42
55	11.43	610	0.69	4.66	I^-/I_3^-	CDCA (1 mM)	42

[a] TiO_2 films were made with 4 μm thick scattering layer. [b] TiO_2 films were made with 8 μm thick scattering layer.

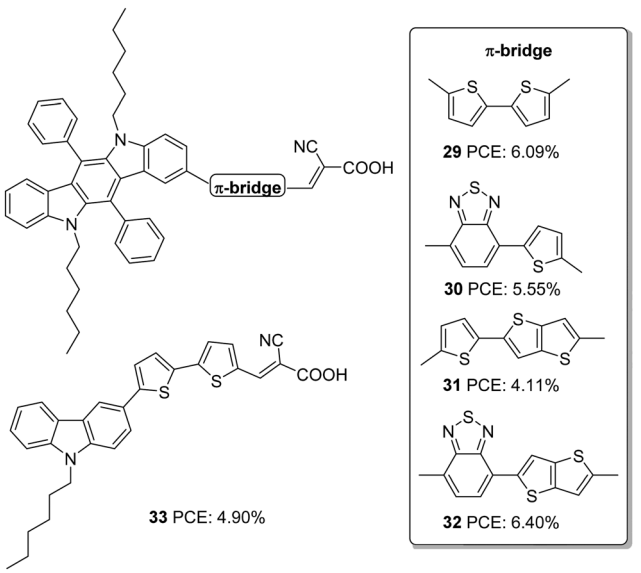

Fig. 9 Photosensitizers with indolo[2,3-*b*]carbazole (**29–32**) and carbazole (**33**) units.

conditions with the least value delivered by **36**. While **35** excelled with the highest PCE of 7.49%, **34** delivered a lower photovoltaic performance of 6.01%. The stability studies reinforced the observation that BTD units are capable of increasing the photo-stability of dyes.

Later in 2016, Qian *et al.* investigated the same donor groups in a new photosensitizer design. They synthesized four dyes utilizing modified donor units (Fig. 11) consisting of indolo[3,2-*b*]carbazole as the primary donor and groups such as ethylbenzene, *N*,*N*-diethylaniline, ethyloxybenzene, and octyloxybenzene grafted to indolo[3,2-*b*]carbazole as secondary donor groups, thiophene as the π-conjugated linker, and 2-cyanoacylic acid unit as the electron acceptor/anchoring group.[36] The secondary donor groups assist in improving the donating strength of the system, but it was also highly beneficial for reducing the aggregation and recombination. Thus the nonplanar secondary groups could enhance the photovoltage of the device. The IPCE performance of the dyes parallels with the electron-donating ability of the secondary donor. The most robust donor, *N*,*N*-diethylaniline attached dye **38**, displayed a broad IPCE response and highest J_{sc} of 15.2 mA cm^{-2} followed by **40**, **39** and **37** (Table 2). The efficiency of the devices also follows the same trend, with **30** having the highest PCE of 8.09%, and the most deficient performance was showcased by **37** with 6.25%.

Later, Xiao *et al.* also employed 6,12-diphenylindolo[3,2-*b*]carbazole as auxiliary donors in D–D–π–A dyes.[37] The sensitizers **41**, **42** and **43** differ in the donor groups: triphenylamine, trimethoxyphenyl and trimethoxybromine, respectively (Fig. 12). Unlike the previous work, the additional donor and π-spacers were appended to the end of the phenylene groups attached to the indolo[3,2-*b*]carbazole moiety. The ICT absorption bands of these compounds did not show much difference compared to the π–π* transition, which can be attributed to the interrupted charge transfer in the molecules resulting from the non-planar conformation of the attached phenyl groups. The absorption behaviour of the compounds was consistent with the electron-donating ability of the secondary donor. The triphenylamine donor in **41**, which has a higher electron-donating ability, contributed to the broader absorption and higher molar extinction coefficient for **41**, followed by **42** and **43**. Though these dyes could deliver reasonably good V_{oc} (0.61–0.75 V) and FF (0.69–0.74) using I^-/I_3^- electrolyte, a relatively low value of J_{sc} resulted in moderate PCE (1.65–3.11%). Dye **41** yielded the highest efficiency of 3.11% followed by **42** and **43** (Table 2).

Further investigations by the same group to increase the photoconversion efficiency of **41** resulted in the synthesis of **44** and **45** where a triphenylamine donor was attached to indolo[3,2-*b*]carbazole *via* the ninth and eighth positions, respectively (Fig. 13).[38] Co-planarity and π-electron delocalization were found to improve, which is apparent from the absorption profile of the new dyes **44** and **45**. Dye **45**, where the phenylene/thiophene rings were connected onto the para positions of the *N*-atom, showed more red-shifted absorption with an absorption maximum at 500 nm, whereas absorption of **44** was blue-shifted by 38 nm. While **44** showed improvement in PCE when it was used in conjunction with CDCA (10 mM), **45** responded in a reverse manner. This can be accounted for by

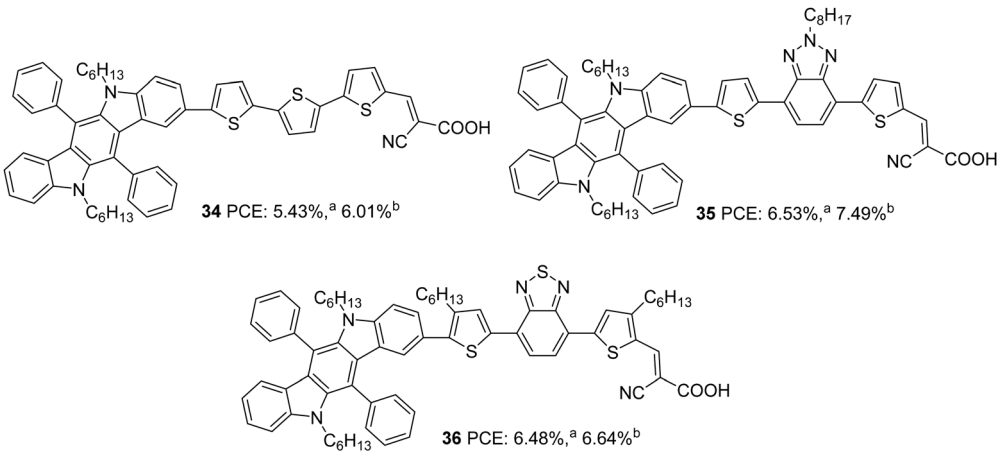

Fig. 10 Photosensitizers **34–36** with an indolo[2,3-*b*]carbazole moiety. [a]TiO_2 films were made with a 4 μm thick scattering layer. [b]TiO_2 films were made with an 8 μm thick scattering layer. In both cases, the active layer was made of 3 μm thick 13 nm particles.

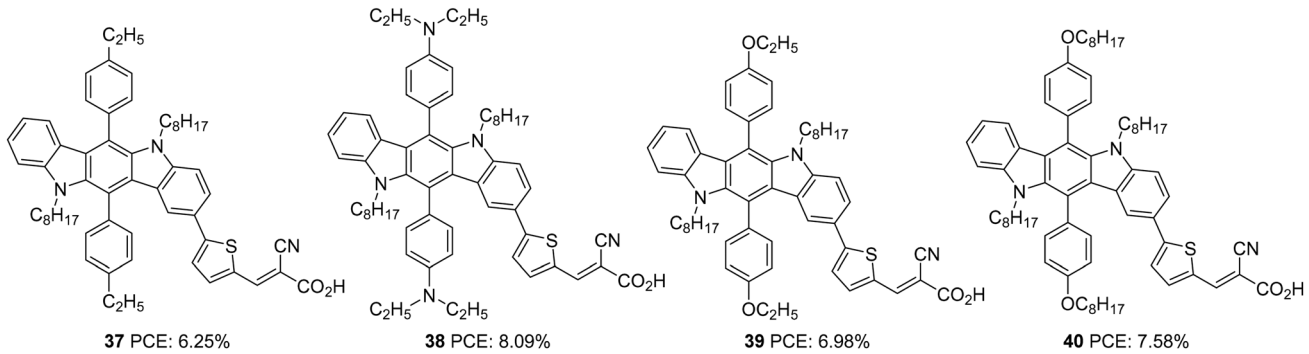

Fig. 11 Photosensitizers **37–40** with an indolo[2,3-*b*]carbazole moiety.

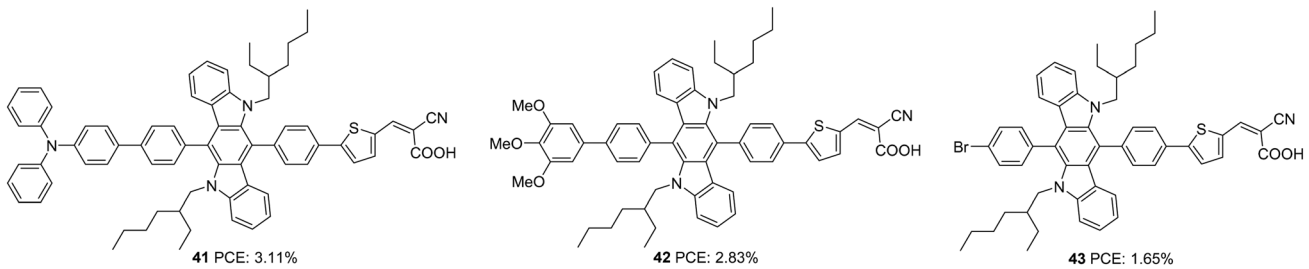

Fig. 12 Photosensitizers **41–43** with an indolo[2,3-*b*]carbazole moiety.

the molecular orientation of the dyes when adsorbed on TiO_2. Dye **44** adopted a perpendicular orientation to the substrate plane. Somewhat hindered conformation of **45** resulted in more inclination of the dye towards the TiO_2 surface. This resulted in fewer aggregations and recombinations, making **45** capable of delivering more photocurrent even with a lower dye loading of 3.64×10^{-7} mol cm^{-2} compared to 4.54×10^{-7} mol cm^{-2} for **44** and without co-adsorbent CDCA. Photosensitizer **45** outperformed **44** with a J_{sc} of 12.85 mA cm^{-2}, V_{oc} of 0.72 V, FF of 0.69 and PCE of 6.34% (Table 2). The co-sensitization of **44**/**45** further improved the performance to 7.03%.

Indolo[2,3-*b*]carbazoles were rarely explored for optoelectronic applications due to a lack of efficient synthetic strategies. Su *et al.* could establish new strategies for synthesising indolo[2,3-*b*]carbazoles and their utilization to construct DSSC sensitizers with a PCE of up to 6.02%.[39] The curved molecular conformation of indolo[2,3-*b*]carbazole dye synthesized by Su *et al.* (**46**), along with its rigid and planar nature, offer the possibility to be explored as a di-anchor dye. The sensitizer **46** adopts A–π–D–π–A architecture in which bithiophene is introduced as the π-bridge between the electron-rich indolo[2,3-*b*]carbazole core and cyanoacrylic acid acceptor unit (Fig. 14). FTIR analysis of the pristine **46**

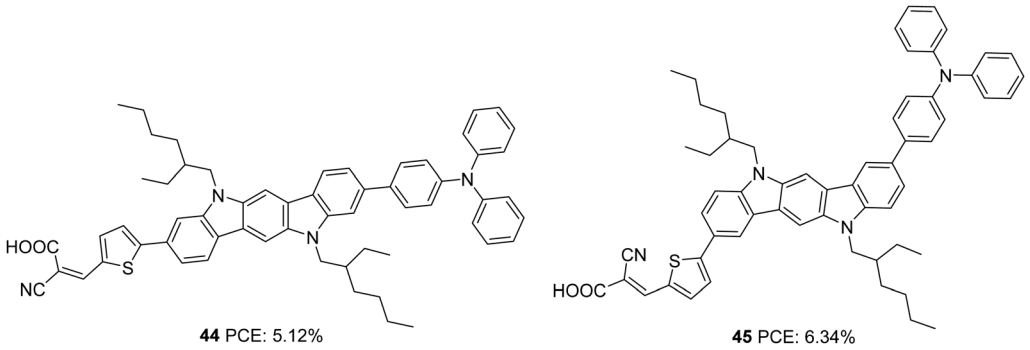

Fig. 13 Photosensitizers **44–45** with an indolo[2,3-*b*]carbazole moiety.

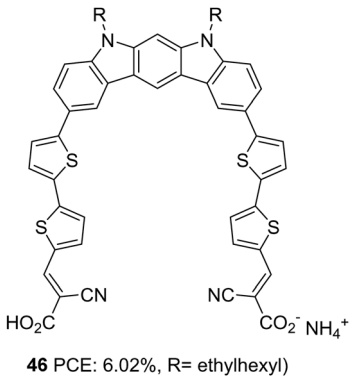

Fig. 14 Molecular structure of photosensitizer **46**.

and the compound loaded TiO_2 film reveals the involvement of both the carboxylic group in anchoring the dye on the TiO_2 surface. This is further confirmed by the Deacon Philips rule, where a frequency difference of 224 cm^1 suggests a bidentate binding mode for **46.** An efficient electron transfer from the HOMO of **46**/$(TiO_2)_{70}$ (indolo[2,3-*b*]carbazole) to the LUMO of **46**/$(TiO_2)_{70}$ (TiO_2 nano cluster) was illustrated using computational analysis.

Indolo[2,3-*a*]carbazole was first introduced in DSSCs by Zhang *et al.*[40] Taking this new system as a donor and cyanoacrylic acid as an acceptor, they studied the effect of conjugate mode of π-spacers such as thienyl-thieno[2,3-*b*]thiophene and terthiophene in photovoltaic performance (Fig. 15). To control dye aggregation and prevent recombination, alkyl-substituted

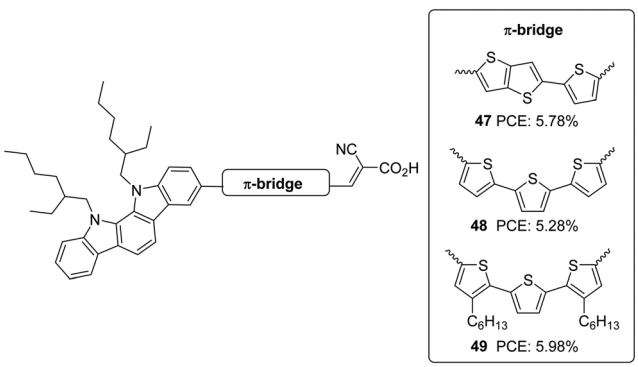

Fig. 15 Photosensitizers **47–49** with an indolo[2,3-*a*]carbazole moiety.

terthiophene was employed as a π-spacer to construct **49**. Sensitizers **47** and **49** outperformed **48** in J_{sc} and V_{oc}. **48** gave an efficiency of 5.28%. The spatial effect of hexyl groups on the π-backbone of **49** resulted in the highest efficiency of 5.98% and the highest photocurrent and photovoltage, followed by **47** with 5.78% PCE (Table 2).

Indolo[3,2,1-*jk*]carbazole is another positional isomer of indolocarbazole where indole is fused with the carbazole moiety in a slightly strained manner. The system was found to be thermostable and showcase strong electron-donating ability, which resulted in its application as a charge transport material and conducting film material. Luo *et al.* utilized this core for developing a sensitizer for DSSCs by integrating it as a donor in a D–π–A architecture (Fig. 16).[41] They developed four devices based on the dyes **50–53**, which exhibited PCE in the range 1.59–3.68%. Among the dyes, **51** outperformed others with a PCE of 3.68% (Table 2). With its lower stabilization energy, thiophene enabled the system to have more delocalization and efficient light-harvesting ability. This can be accounted for by the enhanced photocurrent in dyes **51** and **53** using thiophene as the π-linker. Low spectral coverage leads to decreased performance in **50** and **52**. Even an attempt to increase the π-bridge conjugation by introducing the phenyl group in **52** was not found to be an effective strategy to increase the PCE.

Further attempts were carried out to investigate the effect of π-linkers on the performance of indolo[3,2,1-*jk*]carbazole based dyes by Cao *et al.* (Fig. 17).[42] Dyes **54** and **55** incorporate bisthiophene and unsubstituted bisthiophene, respectively as π-linkers. The slightly twisted conformation of **55** resulted in lower dye loading on TiO_2 than **54**, resulting in a slight increment in the J_{sc} value for **54**, the reverse trend of what was observed for V_{oc}. The significant improvement in J_{sc} of the **54** based device, when adsorbed with CDCA, illustrates the aggregation tendency of these sensitizers on TiO_2. While the **54** based devices delivered PCE of 4.68% in the presence of 10 mM CDCA, dye **55** could yield 4.66% with 1 mM CDCA (Table 2).

Among different isomers of indolocarbazole, indolo[3,2-*b*]-carbazole is the most explored isomer for DSSC applications. The comparison of efficiency *versus* structure reveals that to improve the device's performance, systematic investigation of the position of attachment of the π-spacer and the additional

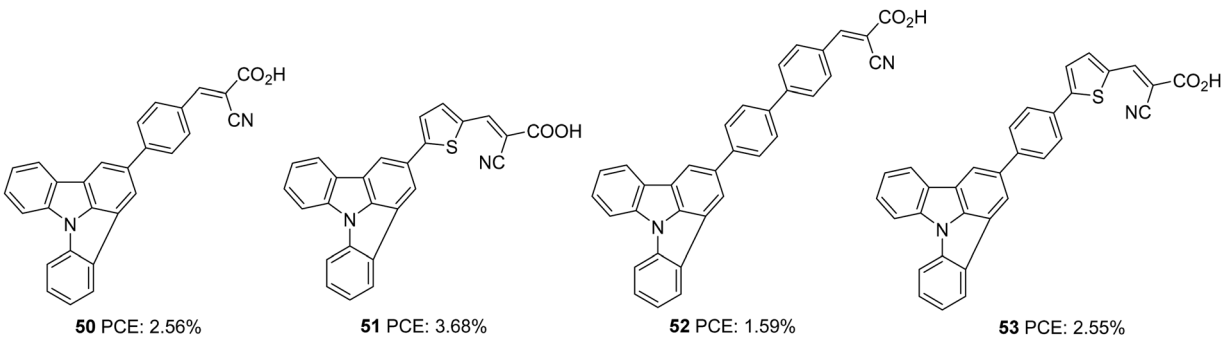

50 PCE: 2.56% **51** PCE: 3.68% **52** PCE: 1.59% **53** PCE: 2.55%

Fig. 16 Photosensitizers **50–53** with an indolo[3,2,1-*jk*]carbazole moiety.

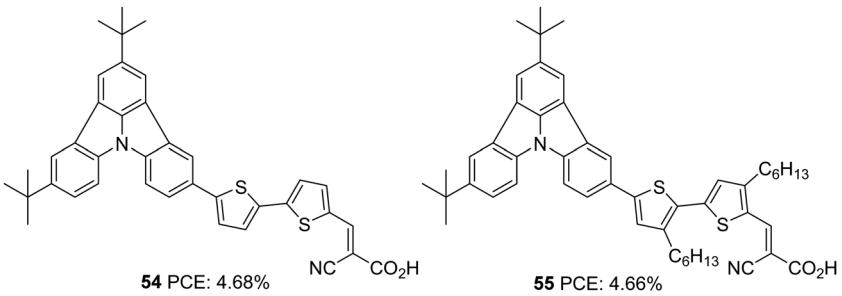

54 PCE: 4.68% **55** PCE: 4.66%

Fig. 17 Photosensitizers **54–55** with an indolo[3,2,1-*jk*]carbazole moiety.

donor on indolo[3,2-*b*]carbazole is also needed, along with the integration of suitable donor and spacer groups. From the reported data so far, the substitution of donor and spacer units at the second and eighth positions of indolo[3,2-*b*]carbazole is more effective than substitution at the ninth and third positions. When the donor group was changed to DDC, the additional phenyl groups integrated at the sixth and twelfth positions were found to prevent recombination while preserving the donating ability and the backbone's planarity. However, attempts to increase the light-harvesting by allowing modifications at these phenyl groups could not lead to realize photovoltaic performance as expected due to the non-planar conformation of the phenyl groups as seen in the case of dyes **41** and **42**.

III. Triazatruxene based sensitizers for DSSCs

Triazatruxene (TAT) is an expanded π-conjugated system with good electron-donating capacity, consisting of three indole units combined using one benzene ring. Due to its favourable features such as electron richness and rigid π-extended structure, it has found application in various optoelectronic fields, like organic field-effect transistors (OFETs), organic light-emitting diodes (OLEDs), two-photon absorption (TPA) materials, nonlinear optics and liquid crystal displays.[43] The most widely used method for the synthesis of TAT is by the reaction between indole and indolone in the presence of bromine and $POCl_3$.[44]

The first attempt to use TAT as a donor in DSSCs was reported by Qian *et al.*[45] They succeeded in developing three D–π–A dyes (**56**, **57**, **58**) with variable π-spacers achieving more than 5% efficiency. These dyes were made using TAT as the donor and cyanoacrylic acid as the acceptor/anchoring group (Fig. 18). The system's efficiency was studied by changing the π-spacers (thiophene **56**, furan **57** and benzene **58**). Though high open-circuit voltage was found in dye **58**, with a reduced current density, devices fabricated with **58** only realized a low PCE of 5.11%. The highest efficiency of 6.1% was contributed by the device fabricated using dye **56**. The higher PCE resulted from higher current density showcased by **56**, which was also evident from the IPCE response (Table 3). Better electron delocalization and superior electron-donating capabilities render the TAT system improved light-harvesting behaviour to be used as an efficient sensitizer in DSSCs.

As an extension of the previous experiments, the effect of rhodanine-3-acetic acid as an electron-withdrawing/acceptor

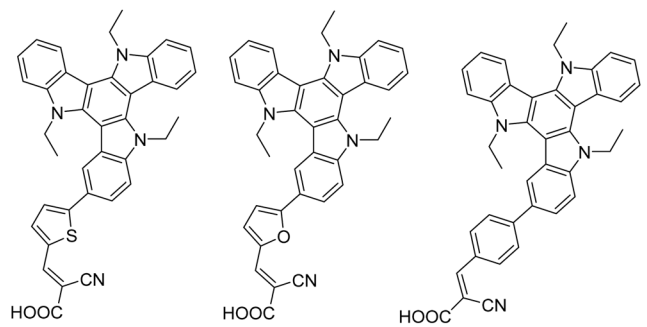

56 PCE: 6.10% **57** PCE: 5.50% **58** PCE: 5.11%

Fig. 18 Photosensitizers **56–58** with a triazatruxene moiety as a donor.

Table 3 Photovoltaic parameters of triazatruxene based DSSCs

Sensitizer	J_{sc} (mA cm^{-2})	V_{oc} (mV)	FF	PCE (%)	Electrolyte	Coadsorbent (concentration)	Ref.
56	14.7	670	0.62	6.10	I^-/I_3^-	—	45
57	13.6	654	0.62	5.50	I^-/I_3^-	—	45
58	11.6	686	0.64	5.11	I^-/I_3^-	—	45
59	5.89	582	0.72	2.47	I^-/I_3^-	CDCA (10 mM)	46
60	8.33	617	0.70	3.60	I^-/I_3^-	CDCA (10 mM)	46
61	14.97	793	0.63	7.5	I^-/I_3^-	CDCA (5 mM)	47
62	16.45	707	0.62	7.15	I^-/I_3^-	CDCA (5 mM)	47
63	13.46	775	0.62	6.50	I^-/I_3^-	CDCA (5 mM)	47
64	15.89	743	0.62	7.26	I^-/I_3^-	CDCA (5 mM)	47
65	11.4	722	0.68	5.55	I^-/I_3^-	CDCA (0.4 mM)	48
66	13.2	741	0.68	6.65	I^-/I_3^-	CDCA (0.4 mM)	48
67	11.0	849	0.53	5.2	I^-/I_3^-	CDCA (0.5 mM)	49
68	20.73	956	0.69	13.6	$[Co(bpy)_3]^{2+/3+}$	CDCA (2 mM)	50
69	20.57	887	0.70	12.8	$[Co(bpy)_3]^{2+/3+}$	CDCA (2 mM)	50
68[a]	9.9	952	0.70	6.6	$[Co(bpy)_3]^{2+/3+}$	CDCA (2 mM)	51
69[a]	8.4	945	0.69	5.4	$[Co(bpy)_3]^{2+/3+}$	CDCA (2 mM)	51
70	11.94	808	0.74	7.20	$[Co(bpy)_3]^{2+/3+}$	CDCA (2 mM)	52
71	15.1	966	0.70	10.2	$[Co(bpy)_3]^{2+/3+}$	—	53
72	13.4	934	0.69	8.6	$[Co(bpy)_3]^{2+/3+}$	—	53
73	16.92	926	0.75	11.7	$[Co(bpy)_3]^{2+/3+}$	—	54
74	15.98	911	0.73	10.6	$[Co(bpy)_3]^{2+/3+}$	—	54

[a] ssDSSC.

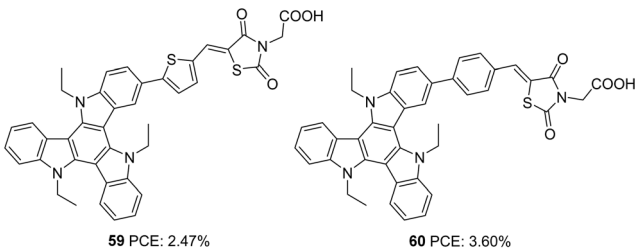

Fig. 19 Photosensitizers **59–60** with a triazatruxene moiety as a donor.

group was studied by the same group (Fig. 19).[46] Though much broader absorption was obtained for dyes with rhodanine-3-acetic acid, the performance of these dyes was inferior to the dyes being synthesized using cyanoacrylic acid as the electron-withdrawing group. This is attributed to the interruption of electron transfer from the dyes to the semiconductor by the broken (NCH_2COOH) conjugation in rhodanine-3-acetic acid. Instead of displaying broader absorption spectra with higher ε, devices fabricated using **59** showed lower current density. The trend can be rationalized from the LUMO energy level of the dyes, which are in the order of **60** (−1.16 V) >**59** (−1.02 V), indicating more effective electron injection from **60** to the semiconductor. Thus **60** could yield a higher PCE of 3.60% with a short-circuit photocurrent density of 8.33 mA cm^{-2}, an open-circuit photovoltage of 617 mV, and a fill factor of 0.70 (Table 3).

Triazatruxene was incorporated as a donor in D–A–π–A based sensitizers by Pan and co-workers in 2018 (Fig. 20).[47] These sensitizers employed benzothiadiazole as an auxiliary acceptor, and they introduced variation in the acceptors (carboxylic acid and cyanoacrylic acid), and the connectivity between the donor and auxiliary acceptor was modified using single bond and ethynyl linkages. The introduction of the ethynyl linker and cyanoacrylic acid was found to increase the conjugation of the dye molecules. Dyes **62** and **64** having cyanoacrylic acid as the acceptor group showed better light-harvesting capability with broader absorption and higher IPCE value. These observations were also reflected in the J_{sc} value of the corresponding sensitizers. Another critical parameter that determines the efficiency of the system is the V_{oc}. Dyes **61** and **63** with a single carboxylic acid acceptor exhibited higher photovoltage compared to the rest. Among the two sets of D–A–π–A sensitizers having a triazatruxene donor (single bonded and ethynyl bridged), dyes **61** and **64** showed maximum efficiencies of 7.51% and 7.26%, respectively, which indicates that a delicate balance between J_{sc} and V_{oc} is essential to obtain higher power conversion efficiencies (Table 3).

Qian and co-workers used triazatruxene as a secondary donor to construct porphyrin-based sensitizers (Fig. 21).[48] Triazatruxene was attached directly to the meso-position of the porphyrin ring, and two variants were synthesized by changing the acceptor groups (carboxylic acid and cyanoacrylic acid). When cyanoacrylic acid was employed as an acceptor group, improvement was found in the dye's light-harvesting ability, which is evident from the broader and enhanced IPCE spectra resulting in a higher J_{sc} value dye (Table 3). The V_{oc} value also follows the same trend, which resulted in a maximum PCE of 6.05% for **66**. The efficiencies of both dyes were found to improve when co-adsorbent chenodeoxycholic acid (CDCA) was used, which implies the possibility of intermolecular aggregation of the dyes on the TiO_2 surface.

Qin *et al.* also incorporated TAT into the meso-position of the porphyrin chromophore to obtain **67** (Fig. 22).[49] Dye **67**, which was used in ssDSSC, with spiro-MeOTAD being the HTM, showcased an efficiency of 5.2% in the presence of co-adsorbent CDCA.

The most efficient DSSC's based on TAT molecules were reported by Zhang and co-workers.[50] They systematically

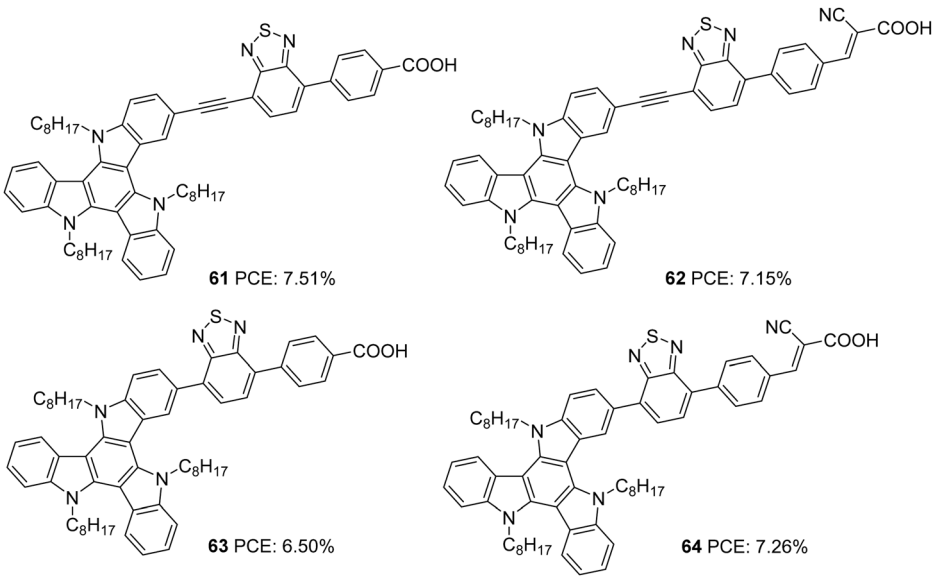

Fig. 20 Photosensitizers **61–64** with a triazatruxene moiety as a donor.

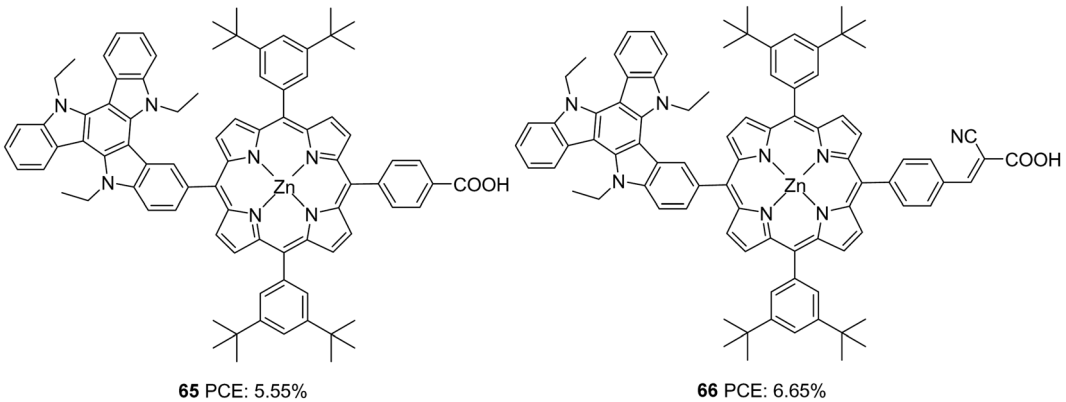

Fig. 21 Photosensitizers **65–66** with a triazatruxene moiety as a secondary donor and porphyrin ring as a primary chromophore.

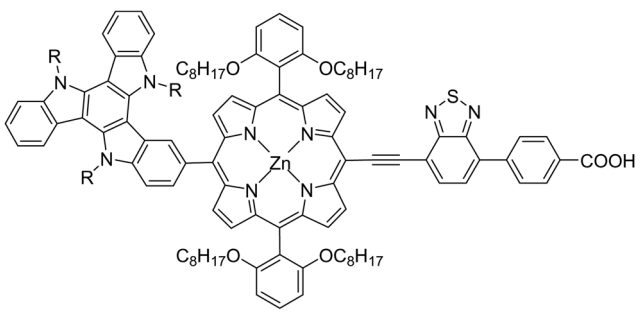

Fig. 22 Photosensitizer **67** with a triazatruxene moiety as a secondary donor and porphyrin ring as the primary chromophore.

modified the D–π–A backbone and developed two dyes employing TAT as a donor, 4,7-bis(4-hexylthiophen-2-yl)benzo[*c*][1,2,5]-thiadiazole (BTBT) as a π-bridge and 4-ethynyl benzoic acid (EBA) as an acceptor, which differs in the linkage between the donor and π-bridge (Fig. 23). The study aimed to evaluate the effect of the rigid single bond and flexible z-type double bond on various parameters that determine the efficiency of the device. The optimized devices based on **68** and **69** achieved PCEs of 13.6% and 12.8%, respectively, using cobalt-based redox electrolyte ($[Co(bpy)_3]^{2+/3+}$). Though the double bond was found to widen and enhance the absorption of the molecules, the J_{sc} value for **68** was found to be higher than **69**, which resulted from the more significant dye loading observed for the former. Devices fabricated using **68** also showcased better open-circuit potential (956 mV) than **69** (887 mV) (Table 3). The efficient electron injection in **68**, evident from the femtosecond transient absorption and up-conversion fluorescence studies, reinforces the observation mentioned earlier. Dye **68** and **69** were also applied to ssDSSCs using spiro-OmeTAD as the hole transporting material (HTM).[51] Longer electron lifetime and high regeneration efficiency caused **68** to outperform **69** with a PCE of 6.6%. Dye **69** exhibited a PCE of 5.4% (Table 3).

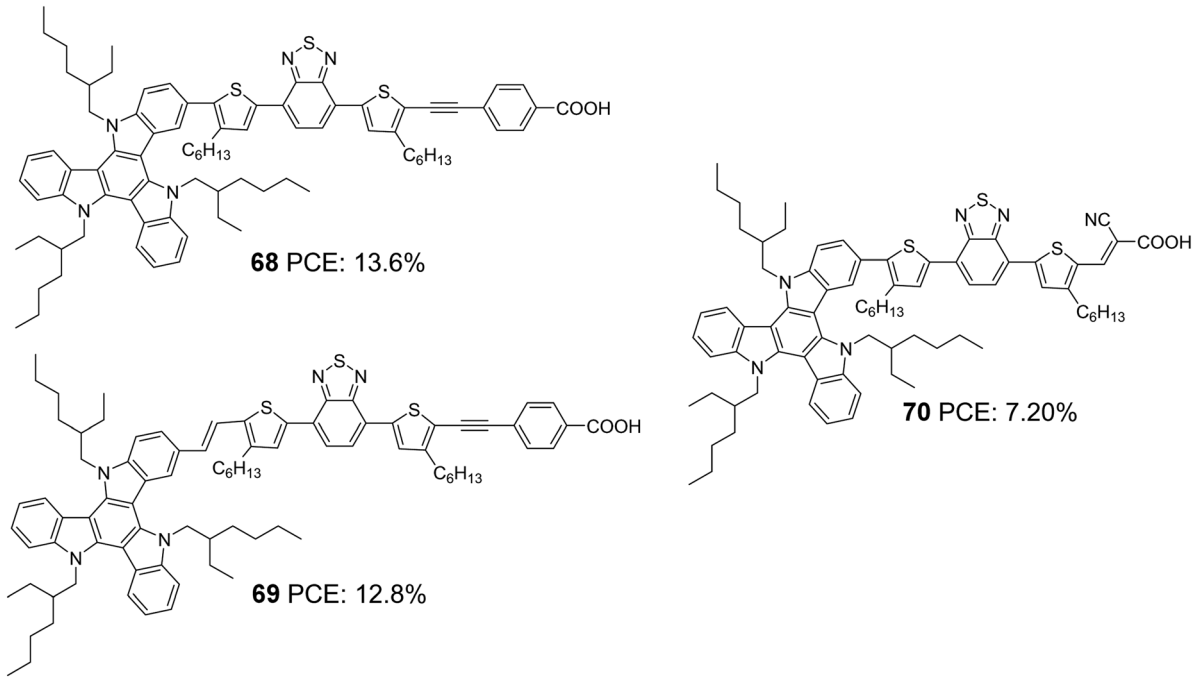

Fig. 23 Photosensitizers **68–70** with triazatruxene moiety as a donor.

In order to probe the effect of the rigid 4-ethynylbenzoic acid acceptor group in **68**, dye **70** was synthesized by the same group (Fig. 23) with Z-type cyanoacrylic acid and used to fabricate devices using a cobalt-based redox electrolyte ($[Co(bpy)_3]^{2+/3+}$).[52] Higher dye loading, better light-harvesting ability and improved electron injection efficiency made **68** deliver the highest efficiency of 13.4%, while there was a drastic drop in PCE for **70**, which could only afford a PCE of 7.2% (Table 3). This again clearly illustrates that rigid structures are pertinent when it comes to designing sensitizers that will be beneficial for reducing energy loss during electron injection, leading to improved current density and photovoltage. Fine-tuning of the molecular backbone without compromising the energetics is highly required to realize higher PCE.

Later, Li *et al.* tried to improve the efficiency of **68** by developing two modified dyes **71** and **72** using a TAT donor (Fig. 24).[53] While benzothiadiazole (BT) functions as the auxiliary acceptor in **71**, BT was replaced with difluorobenzo[*c*][1,2,5]-thiadiazole (DFBT) in **72**. The attempt to introduce fluorine on BT was justified by lowering the LUMO level of the molecule by the electron-withdrawing (inductive) effect of fluorine. The electron-donating mesomeric effect was found to dominate the former. This renders **72** with a large band gap and blue-shifted absorption spectrum compared to that of **71**. The higher dye loading in **71** (1.4 times) and wider absorption band compensated the reduction in molar extinction coefficient, resulting in a higher J_{sc} of 15.1 mA cm^{-2}. This ended up in maximum efficiency of 10.2% for **71** and a lower efficiency of 8.6% for **72** using cobalt-based redox electrolyte ($[Co(bpy)_3]^{2+/3+}$). (Table 3).

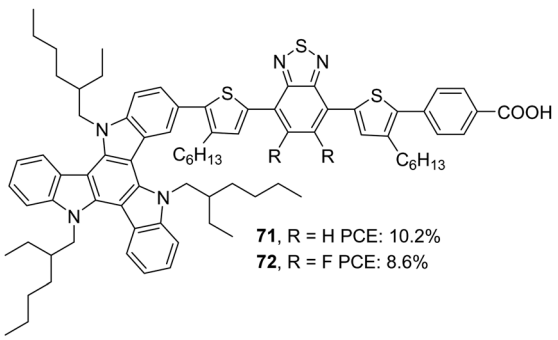

Fig. 24 Photosensitizers **71–72** with a triazatruxene moiety as a donor.

Yao *et al.* found that introducing bulky groups on TAT successfully hindered dye aggregation and recombination (Fig. 25).[54] They synthesized two modified TAT sensitizers (**73** and **74**) having a more conjugated TAT donor unit. Their attempt resulted in a larger V_{oc} for **73** (926 mV) and **74** (911 mV). Higher dye loading in **73** compared to **74** allowed adequate coverage of the semiconductor surface, abating the chances of dark current formation (recombination), leading to higher V_{oc}. DFT studies also revealed more planar conformation for **74** than **73**, which confirms the slightly red-shifted absorption profile of **74**. It was also observed that there was an upshift in HOMO level for **74**, which affected the regeneration rate of the dye adversely. Poor regeneration and lower dye loading resulted in lower current density and V_{oc} for **74** compared to **73**. Thus, PCEs of 11.7% and 10.6% were obtained for **73** and **74**, respectively (Table 3).

Triazatruxene was incorporated as a donor in D–π–A dyes and studies were carried out to evaluate the effect of different π-spacers and anchoring groups. When it comes to the anchoring group, cyanoacrylic acid has proved to outperform other

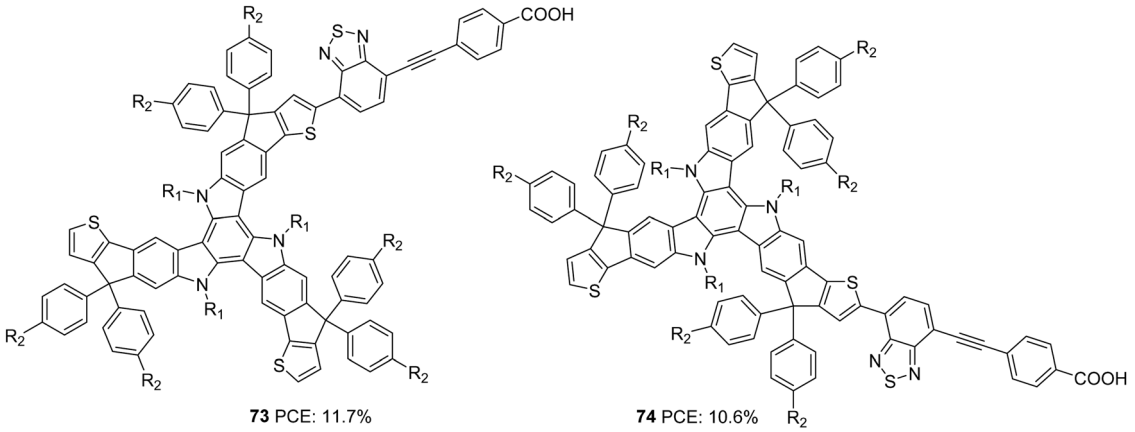

Fig. 25 Photosensitizers **73–74** with a triazatruxene moiety as a donor.

acceptor units (rhodanine-3-acetic acid, carboxylic acid) in terms of light-harvesting and electron injection capability, which is consistent with the many reports available. Though devices based on thiophene bridged dye **56** could showcase higher PCE than those of phenyl substituted dye **58**, this trend reverses when the anchoring group was changed to rhodanine-3-acetic acid. Devices fabricated with phenyl bridged dye **60** delivered higher PCE with higher J_{sc} and V_{oc} compared to those of **59** with a thiophene spacer. This implies that selecting a suitable π-spacer depends on the other components of the molecular architecture. The introduction of an auxiliary acceptor improved the photovoltaic parameters, and the highest efficiency achieved so far using metal-free dyes is from devices based on **68** (13.6%) where BTBT was used as the π-bridge (Table 3). The takeaway from the consecutive studies performed by Zang and co-workers is that molecular engineering has to be carried out in such a way as to reduce energy loss during electronic transitions, which could, in turn, lead to efficient PCE.

IV. Indeno[1,2-*b*]indole based sensitizers for DSSCs

Indeno[1,2-*b*]indole consists of an indole unit fused with an indene moiety, making it planar and electron-rich with efficient electron delocalization. In addition to the alkylation of the N-atom in the tetracene, the indene unit also offers the flexibility to be alkylated. This possibility has a positive effect on the photovoltaic performance as the presence of multiple alkyl groups increases the solubility of indeno[1,2-*b*]indole based dyes and prevents their aggregation. At the same time, the presence of alkyl groups is also effective in blocking the approach of the oxidized species coming close to the semiconductor and thereby improving lifetime. The well-established synthetic route towards preparing this tetracene is by the Fisher indole synthesis involving indanone and phenyl hydrazine.[55]

The first report on the use of indeno[1,2-*b*]indole as a donor in a DSSC came in 2016 by Qian *et al.*[56] They designed four dyes (Fig. 26) based on D–π–A design, and the basic skeleton employs indeno[1,2-*b*]indole as a donor and cyanoacrylic acid

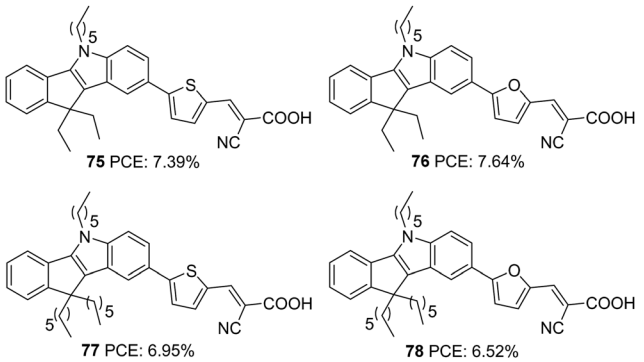

Fig. 26 Photosensitizers **75–78** with an indeno[1,2-*b*]indole moiety as a donor.

as the acceptor. Tuning of device performance was carried out by changing the π bridges (furan and thiophene) and introducing alkyl groups (ethyl and hexyl) on the indene ring. The attached alkyl groups were at a particular angle with the molecular plane, which was beneficial for reducing aggregation of dyes and thereby increasing the PCE. All four dyes exhibited good power conversion efficiency in the range 6.52–7.64%. Among these dyes, the sensitizer **76**, featuring furan as the π-spacer and ethyl groups as the alkyl chain, contributed the highest PCE of 7.64% with a J_{sc} of 15.8 mA cm^{-2} and a V_{oc} of 763 mV (Table 4).

Qian and co-workers later designed three more dyes with indeno[1,2-*b*]indole as the donor to investigate the role of different acceptor groups on the photovoltaic performance of the devices.[57] The synthesized D–π–A dyes had indeno[1,2-*b*]-indole as a donor and benzene as the π-bridge. The dyes differed in the acceptor groups incorporated, which were cyanoacrylic acid, rhodanine-3-acetic acid and 2-(1,1-dicyanomethylene)-rhodanine (DCRD), respectively (**79**, **80** and **81**) (Fig. 27). The results revealed better PCE for devices fabricated using dye having cyanoacrylic acid as the acceptor over the other two groups. Though dye **79** showed blue-shifted absorption, it contributed towards the highest efficiency of 6.29% with better J_{sc} and V_{oc} compared to other dyes. To assess the effect of different π-spacers on the DCRD acceptor, dye **82** was synthesized with thiophene as the π-bridge. The introduction of thiophene increased the

Table 4 Photovoltaic parameters of indenoindole based DSSCs

Sensitizer	J_{sc} (mA cm^{-2})	V_{oc} (mV)	FF	PCE (%)	Electrolyte	Coadsorbent (concentration)	Ref.
75	15.6	710	0.67	7.39	I^-/I_3^-	—	56
76	15.8	763	0.63	7.64	I^-/I_3^-	—	56
77	14.6	742	0.64	6.95	I^-/I_3^-	—	56
78	13.7	733	0.65	6.52	I^-/I_3^-	—	56
79	11.0	813	0.70	6.29	I^-/I_3^-	—	57
80	4.23	700	0.75	2.22	I^-/I_3^-	—	57
81	7.10	695	0.73	3.60	I^-/I_3^-	—	57
82	11.9	707	0.64	5.41	I^-/I_3^-	—	57
83	10.4	843	0.66	5.74	I^-/I_3^-	CDCA (3 mM)	58
84	13.3	796	0.65	6.86	I^-/I_3^-	CDCA (3 mM)	58
85	14.1	829	0.68	7.99	I^-/I_3^-	CDCA (3 mM)	58
84/85	14.7	819	0.70	8.37	I^-/I_3^-	—	58
86	18.25	707	0.68	8.74	I^-/I_3^-	—	59
87	20.08	703	0.64	8.98	I^-/I_3^-	—	59
88	12.01	837	0.69	6.92	I^-/I_3^-	—	59
86/88	18.24	787	0.67	9.56	I^-/I_3^-	CDCA (4 mM)	59
89	11.59	840	0.66	6.43	$[Co(phen)_3]^{2+/3+}$	—	60
90	6.84	770	0.63	3.31	$[Co(phen)_3]^{2+/3+}$	—	60
91	12.43	829	0.65	6.69	$[Co(phen)_3]^{2+/3+}$	—	60
92	13.52	855	0.64	7.40	$[Co(phen)_3]^{2+/3+}$	—	60

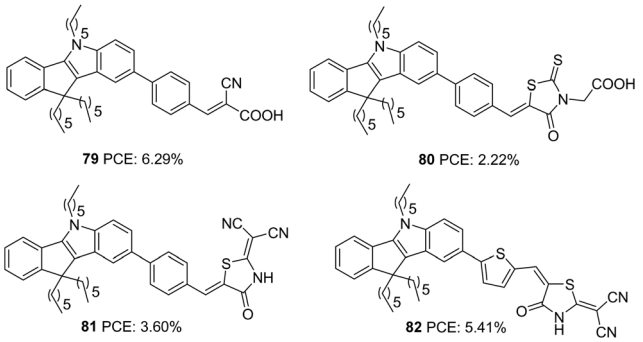

Fig. 27 Photosensitizers **79–82** with an indeno[1,2-*b*]indole moiety as a donor and variable acceptor groups.

efficiency of **81** from 3.60% to 5.41%, illustrating the importance of tuning the π-spacer of the sensitizer (Table 4) while changing the acceptor functionality in a way to achieve higher PCE.

Yan *et al.* later designed and synthesized indeno[1,2-*b*]-indole based D–π–A dyes with extended conjugation of the π-spacer by introducing an ethynyl group and variation of the π-spacer and auxiliary acceptor. To this end, they constructed D–π–A dyes, which employ indeno[1,2-*b*]indole as the donor and cyanoacrylic acid as the acceptor group (Fig. 28).[58] The dyes **83** and **84** vary in the π-bridge between benzene and thiophene, respectively. They also incorporated the ethynyl group as the linker between the donor and π-spacer to decrease the repulsion and increase the conjugation of the dye molecules. A third dye, **85** with benzothiadiazole as the auxiliary acceptor, was developed to compare with the previous set realizing D–π–A architecture. The dye with an auxiliary acceptor (**85**) was found to deliver the highest efficiency with the highest J_{sc} and V_{oc}. Among the D–π–A dyes, thiophene substituted dye **84** showed the highest efficiency with significantly improved current density, though V_{oc} was highest for the benzene substituted dye **83**. Co-sensitization of **84** and **85** outperformed all other dyes delivering an efficiency of 8.37% (Table 4). This is attributed to the increment in the J_{sc} value of the device.

Dai and co-workers first synthesized indeno[1,2-*b*]indole-spirofluorene (IISF) and used it as a donor unit in DSSC dyes. This molecular engineering was carried out to combine the electron-donating ability of the indenoindole with the steric effect of the spirofluorene.[59] They were successful in developing two dyes, **86** and **87**, with IISF as the donor, dithieno[3′,2′-*b*:2′,3′-*d*]pyrrole (DTP) as the π-bridge and cyanoacrylic acid as an acceptor (Fig. 29). The dye **87** also employs 2,1,3-benzothiadiazole (BTD) as an auxiliary acceptor. Both **86** and **87** delivered efficiencies above 8%, which was further enhanced with the combined effect of co-adsorption with CDCA and co-sensitization with **88**. The highest efficiency of 9.56% was obtained from the co-sensitization of **86** with **88** in the presence of co-adsorbent, CDCA (Table 4).

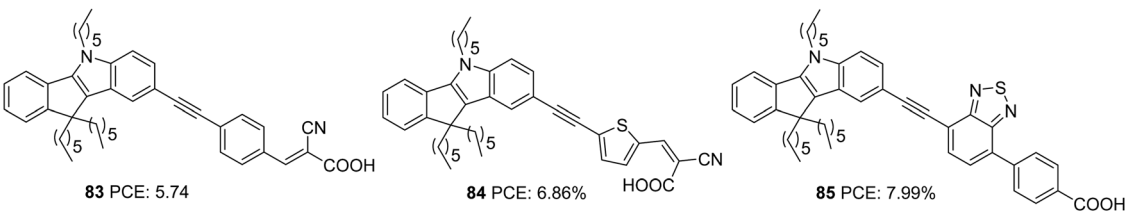

Fig. 28 Photosensitizers **83–85** with an indeno[1,2-*b*]indole moiety as a donor.

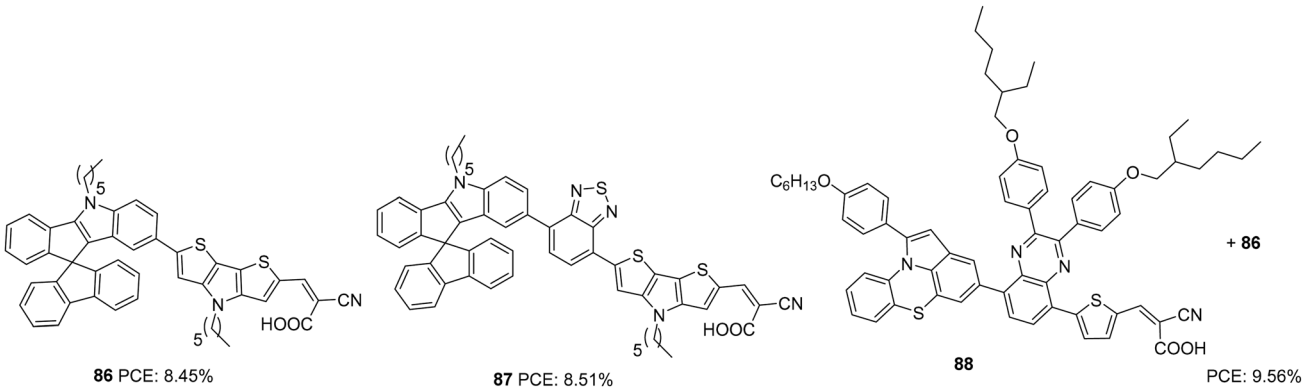

Fig. 29 Photosensitizers **86–87** with an indeno[1,2-*b*]indole-spirofluorene moiety as a donor.

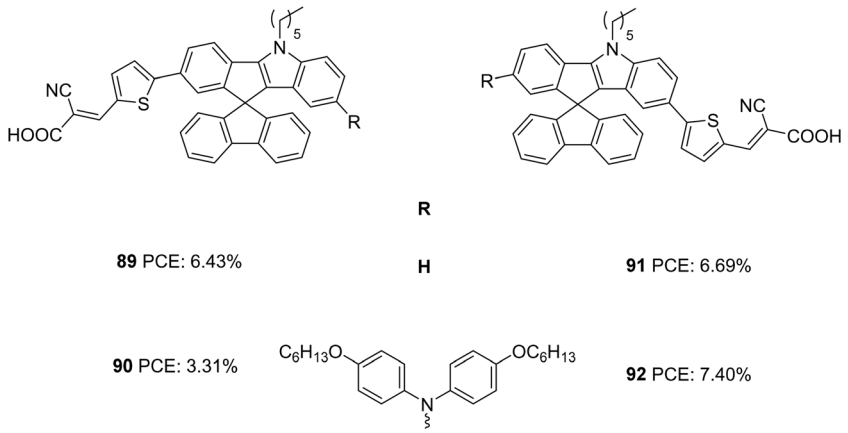

Fig. 30 Photosensitizers **89–92** with an indeno[1,2-*b*]indole-spirofluorene moiety as a donor.

Later the same group synthesized two sets of dyes based on IISF to study the effect of position of attachment of the π-spacer to IISF (indole/indene end) and the effect of the additional donors (Fig. 30).[60] The D–π–A dyes **89** and **91** consist of IISF as the donor, thiophene as the π-spacer and cyanoacrylic acid as the acceptor. While thiophene is attached to the indene ring in **89**, dye **91** has the π-spacer attached to the indole end. An additional donor group (hexyloxydiphenylamine) was attached to **89** to obtain **90**, and dye **92** is the latter's regioisomer. Dyes with additional donors exhibited bathochromic as well as intensified spectra compared to D–π–A dyes. Among the two regioisomers, the one with the π-spacer attached to the indole end of IISF is seen to facilitate more ICT transition. The IPCE spectra of **90** and **92** showed wider but downshifted absorption behaviour than **89** and **91**. A higher adsorption angle of **89** (41.83°) and **91** (42.33°) helped them to achieve higher dye loading of 115.83 and 118.14 nmol cm^{-2}, respectively. The bulkier donor group in **90** and **92** caused decreased dye loading compared to their D–π–A counterpart, but **92** managed to obtain 77% dye loading of **91** due to its larger adsorption angle (49.5°). Though dye loading was lower for **92** (90.97 nmol cm^{-2}) than **89** and **91**, the broader absorption could compensate for it having the highest J_{sc} (13.52 mA cm^{-2}). While **89** and **91** exhibited comparable J_{sc} of 11.59 and 12.43 mA cm^{-2}, respectively, **90** delivered the least J_{sc} value of 6.84 mA cm^{-2}. Apart from the lower dye loading, the weak driving force for degeneration also caused the downfall in current density for **90.** This was again illustrated by changing alternate electrolytes for device fabrication which are having lower oxidation potential than $[Co(phen)_3]^{2+/3+}$([0.56 V for $Co(bpy)_3]^{2+/3+}$, and 0.43 V for $[Co(dmbpy)_3]^{2+/3+}$). The current density of **90** increased in the order $[Co(dmbpy)_3]^{2+/3+} > [Co(bpy)_3]^{2+/3} > [Co(phen)_3]^{2+/3+}$. While the bulky hexyloxy diphenyl helped **92** alleviate recombination and achieve higher V_{oc}, the same group adversely affected the V_{oc} in **90** by breaking the compact layer formed by dye **89**. A trade-off between J_{sc} and V_{oc} in **89** and **91** lead to comparable efficiencies for them. While **92** showcased the highest PCE of 7.40%, dye **90** delivered the lowest PCE of 6.84%. Co-sensitization of **92** was carried out with **89**/**91**. In both cases, increment in current density was observed, **91**/**92** being the combination with the highest PCE (8.32%)

On comparing the sensitizers **77**, **78** and **79** having the same dye skeleton and differing only in their π-spacer, sensitizer **77** having thiophene as the π-spacer outperformed the rest of the dyes with higher current density. Though sensitizer **79** has higher V_{oc}, the least PCE was delivered due to lower current density. A triple bond was introduced between the indenoindole

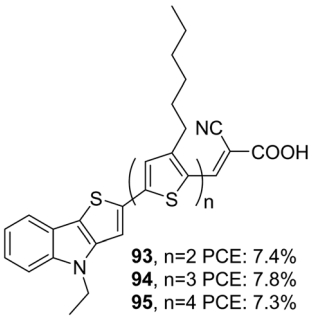

Fig. 31 Photosensitizers **93–95** with a thieno[3,2-*b*]indole moiety as a donor.

unit and π-spacer in **77** and **79** to furnish **84** and **83**. Though the motive was to increase the conjugation and PCE of the devices, it was found to showcase low PCE compared to its predecessor. Though the new structure could bring about an increment in V_{oc}, current density followed the reverse trend.

V. Thieno[3,2-*b*]indole (TI) and thieno[2,3-*b*]indole based sensitizers for DSSCs

In thieno[3,2-*b*]indole (TI), an electron-rich system like thiophene is fused to the five-membered ring of the indole moiety at the 2–3 positions. It has been proved that thieno[3,2-*b*]indole is a better donor than both indole and carbazole units. The introduction of thieno[3,2-*b*]indole as a component in the dye design would certainly improve photovoltaic performance due to the co-planarity and strong electron-donating ability of these heteroacenes. The thieno[3,2-*b*]indole moiety can be easily synthesized using a Cadogen reaction of suitable functionalized 2-(2-nitrophenyl)thiophene.[61]

The first report of a thieno[3,2-*b*]indole based DSSC was reported by Zang *et al.* in 2010.[62] They synthesized three dyes (**93**, **94** and **95**) employing 4-ethyl-4*H*-thieno[3,2-*b*]indole moiety as an electron donor, *n*-hexyl substituted oligothiophene units as a π-spacer and cyanoacrylic acid as an electron acceptor/anchoring group (Fig. 31). A comparison was also made with dyes having *N*-ethyl carbazole, which consists of the same dye skeleton.[63] The electron lifetime measurement values obtained for the TI based devices are lower than their parent D–π–A carbazole dyes, leading to lower V_{oc} for these devices, having the least value of 660 mV for the **95** based device. According to the DFT calculations, the dihedral angle between the thienyl group and the donor part is found to be less for TI based sensitizers in comparison to that of carbazole dyes. This increase in planarity and better electron-donating capability is reflected in the broader absorption spectra and higher ε values displayed by dyes employing thieno[3,2-*b*]indole as the donor unit. This resulted in an increment in current density, which was in line with the increment in the number of thiophene groups in the π-backbone. Among the TI dyes, **94** exhibited a higher PCE of 7.8%, and the minor performance was delivered by **95** (7.3%) (Table 5). An increase in the number of thiophene moieties resulted in higher HOMO levels for **95**. Though this tendency could produce low bandgap sensitizers with better light-harvesting, a decrease in driving force for dye regeneration and the chances of recombination of injected electrons with the oxidized dyes may be responsible for decelerating the performance of **95**.

The role of thieno[3,2-*b*]indole (TI) as a π-spacer was demonstrated successfully by Kim and co-workers.[64] In their initial work, they designed and synthesized D–A–π–A sensitizers using TI (**97**, **98**) as a π-spacer and a comparative investigation was made between dyes with thieno[3,2-*b*]benzothiophene (TAB) as a π-spacer (**96**) (Fig. 32). The more electron-donating nature of TI could induce effective charge transfer in **97** and **98** with resultant wider absorption behaviour and ε-values compared to those of **96**. These molecules also exhibited effective electron injection efficiency, with **98** being the best performer with improved light-harvesting ability. The IPCE performance of

Table 5 Photovoltaic parameters of thieno[3,2-*b*]indole and thieno[2,3-*b*]indole based DSSCs

Sensitizer	J_{sc} (mA cm^{-2})	V_{oc} (mV)	FF	PCE (%)	Electrolyte	Coadsorbent (concentration)	Ref.
93	13.8	700	0.77	7.4	I^-/I_3^-	—	62
94	14.6	700	0.76	7.8	I^-/I_3^-	—	62
95	15.0	660	0.74	7.3	I^-/I_3^-	—	62
96	16.84	810	0.72	9.83	$[Co(bpy)_3]^{2+/3+}$	CDCA (20 mM)	64
97	18.35	804	0.75	11.04	$[Co(bpy)_3]^{2+/3+}$	CDCA (20 mM)	64
98	19.39	825	0.74	11.84	$[Co(bpy)_3]^{2+/3+}$	CDCA (20 mM)	64
99	16.39	834	0.75	10.2	$[Co(bpy)_3]^{2+/3+}$	HC-A1 (0.6 mM)	65
100	17.15	839	0.74	10.5	$[Co(bpy)_3]^{2+/3+}$	HC-A1 (0.6 mM)	65
101	17.12	849	0.73	10.6	$[Co(bpy)_3]^{2+/3+}$	HC-A1 (0.6 mM)	65
102	17.49	898	0.72	11.4	$[Co(bpy)_3]^{2+/3+}$	HC-A1 (0.6 mM)	65
103	15.62	759	0.76	9.05	$[Co(bpy)_3]^{2+/3+}$	HC-A1 (6 mM)	66
104	16.42	846	0.77	10.69	$[Co(bpy)_3]^{2+/3+}$	HC-A1 (6 mM)	66
105	16.50	847	0.77	10.80	$[Co(bpy)_3]^{2+/3+}$	HC-A1 (6 mM)	66
106	1.06	490	0.73	0.37	$[Co(bpy)_3]^{2+/3+}$	—	68
107	3.2	360	0.69	0.79	$[Co(bpy)_3]^{2+/3+}$	—	68
108	19.0	590	0.56	6.3	$[Co(bpy)_3]^{2+/3+}$	—	69
109	19.9	390	0.44	3.4	$[Co(bpy)_3]^{2+/3+}$	—	69
110	4.7	470	0.61	1.3	$[Co(bpy)_3]^{2+/3+}$	—	69
111	6.6	370	0.56	1.4	$[Co(bpy)_3]^{2+/3+}$	—	69

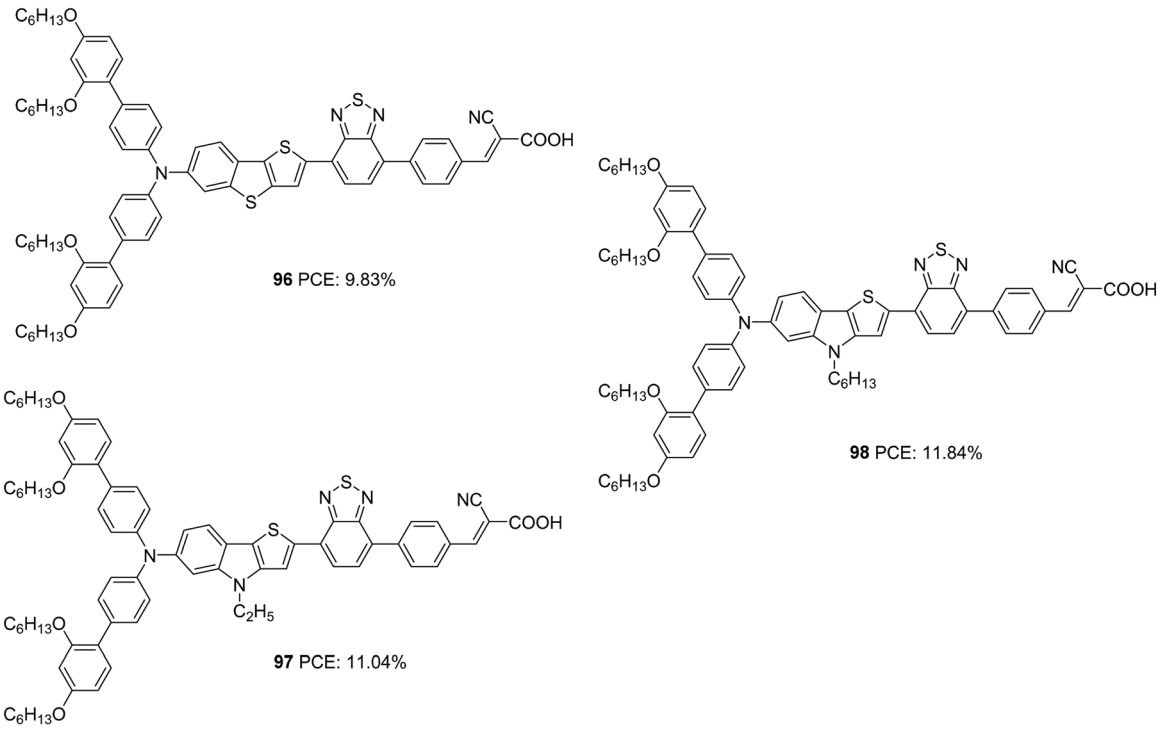

Fig. 32 Photosensitizers with a thieno[3,2-*b*]indole moiety (**97**, **98**) and thieno[3,2-*b*] benzothiophene (**96**) as a π-spacer.

the dyes parallels these observations leading to the highest J_{sc} for **98** (19.39 mA cm^{-2}) followed by **97** (18.35 mA cm^{-2}) and **96** (16.84 mA cm^{-2}). The hexyl chain was found to minimize the dye aggregations effectively in **98** with lesser recombination, which resulted in a higher V_{oc} (825 mV) for the same (Table 5). The trends described above in device parameters ended in highest PCE for **98** (11.84%) followed by **97** (11.04%) and **96** (9.83%) using CDCA co-adsorbent and cobalt electrolyte ($[Co(bpy)_3]^{2+/3+}$).

Later the same group synthesized **99–102.** The objective was to reduce the aggregation-induced recombination occurring in devices fabricated with **98.** The donor group in **98** was substituted with fluorenyl derivatives with the other building blocks remaining unchanged using D–A–π–A architecture with BTD as an auxiliary acceptor and cyanoacrylic acid as an acceptor/anchoring group (Fig. 33).[65] The synthesized dyes **99–102** employ bis(9,9-dimethyl-9*H*-fluoren-2-yl)amino (FA),[20] bis(6,7-bis(hexyloxy)-9,9-dimethyl-9*H*-fluoren-2-yl)amino (HFA), bis(6,7-bis(decyloxy)-9,9-dimethyl-9*H*-fluoren-2-yl)amino (DFA), and bis(7-(2,4-bis(hexyloxy)phenyl)-9,9-dimethyl-9*H*-fluoren-2-yl)amine (BBFA) groups respectively as donors. To encounter solubility problems associated with the fluorene derivatives, all the devices were made with a change in dipping solvent resulting in lower PCE (10.5%, J_{sc}: 16.67 mA cm^{-2}, V_{oc}: 840 mV, FF: 0.75) for **98** than previously reported. All the devices were found to exhibit improved performance when the electrolyte was changed from iodide/triiodide to cobalt-based electrolyte ($[Co(bpy)_3]^{2+/3+}$) and in the presence of HC-A1 as the co-adsorbent. The alkoxy, as well as phenyloxy substituted fluorene derivatives (**100–102**), were found to be more effective both in red shifting the absorption spectrum as well as in preventing recombination, taking advantage of the electron-donating as well as the bulkiness of the donor groups, when compared to FA substituted dye **99.** This lead to higher current density and photocurrent for **100–102** resulting in higher PCE. Though **99** does not have additional alkoxy substitutions integrated on it, the absorption profile shows a redshift when compared to those of **98** having

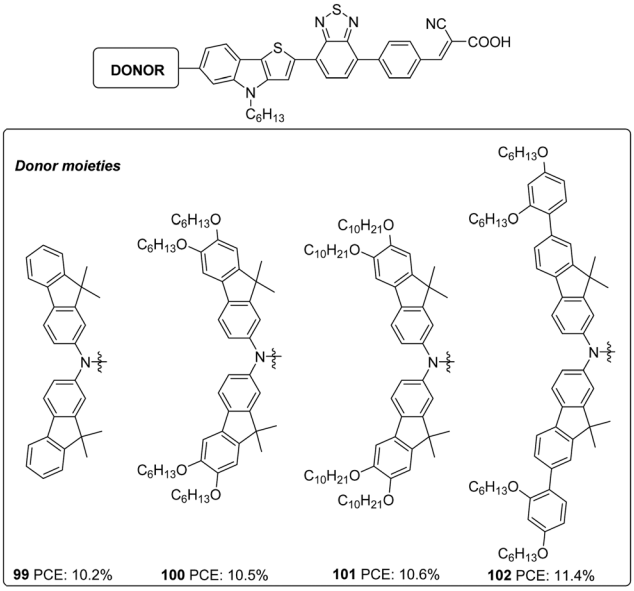

Fig. 33 Photosensitizers **99–102** with thieno[3,2-*b*]indole moiety as the π-spacer.

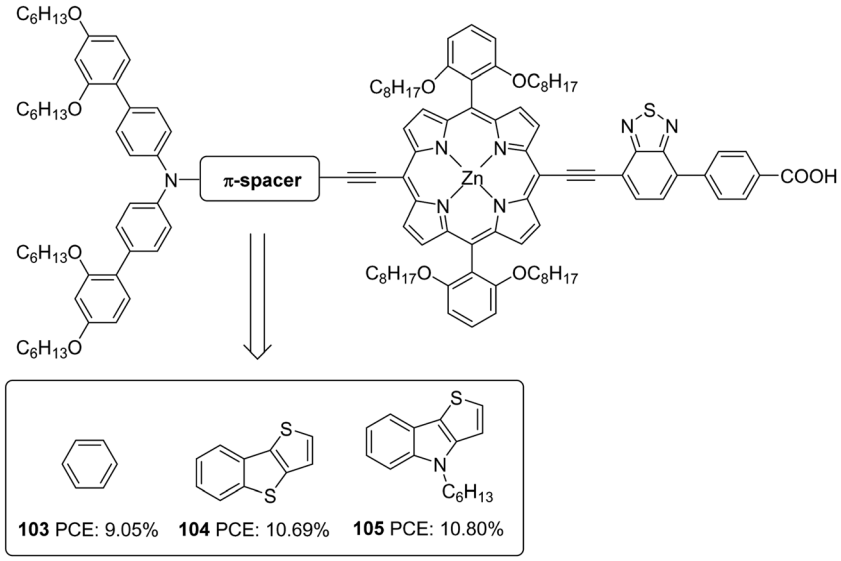

Fig. 34 Molecular structures of photosensitizers **103–105** with different π-spacers.

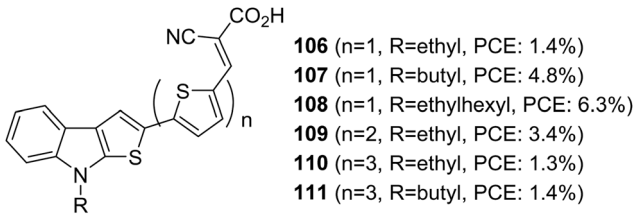

Fig. 35 Photosensitizers **106–111** with thieno[3,2-*b*]indole moiety as the donor.

BBPA (bis(2′,4′-bis(hexyloxy)-[1,1′-biphenyl]-4-yl)amino) as the donor. This absorption behaviour can be accredited to a lack of electronic communication between the alkoxy groups and the tertiary amine in BBPA based dye **98**. A higher molar extinction coefficient of **98** contributed towards higher current density compared to **99**. The bulkier BBPA also rendered **98** to have higher V_{oc} and hence higher PCE when compared to those of **99**. The device fabricated based on **102** showcased the highest efficiencies of 11.4%, and **99** delivered the least efficiency of 10.2% (Table 5).

The superior performance of TI over TAB as a π-conjugator was again illustrated by Ji *et al.* (Fig. 34).[66] To this end, two porphyrin based D–π–A dyes (D-ethynyl-zinc porphyrinyl-ethynyl-benzothiadiazole-acceptor) with extended conjugation at the donor sites were constructed. The dyes **104** and **105** differ in the auxiliary spacer between thieno[3,2-*b*]benzothiophene (TBT) and 4-hexyl-4*H*-thieno[3,2-*b*]indole, and were also subjected to a comparison with phenylethylene based dye **103** from earlier work.[67] The dihedral angle between the donor part and π-spacer showed increment when the phenyl group in **103** was replaced with TI and TAB units with more conjugation. The trend observed in V_{oc} was following the increase in dihedral angle (**105** > **104** > **103**), which might have helped prevent the recombination effectively. The more electron-donating TI and TAB groups could also bring changes in the light-harvesting ability of the dyes. In the Q-bands, significant changes were observed, having a more expansive and intensified absorption profile for **104**–**105**, leading to current densities in the order **105** > **104** > **103**. The more planar, electron-donating nature of the TI group along with the incorporated hexyl functionality contributed towards the best efficiency of 10.80% for **105** with higher J_{sc} (16.50 mA cm^{-2}) and V_{oc} (0.847 V) (Table 5) in the presence of HC-A1 as the co-adsorbent, using $[Co(bpy)_3]^{2+/3+}$ (bpy = 2,2′-bipyridine) redox electrolyte.

Thieno[2,3-*b*]indole was applied as a building block in DSSCs for the first time by Irgashev *et al.* (Fig. 35).[68,69] They introduced a new synthetic route for constructing thieno[3,2-*b*]-indole from 1-alkylisatin and 2-acetylthiophene. Among the dyes, **108** with thiophene as the π-bridge and ethyl hexyl as the alkyl group contributed towards the highest PCE of 6.3%. The bithiophene and terthiophene groups were entertaining aggregation of dyes which resulted in more recombination. Except for ethyl hexyl, other smaller alkyl groups like butyl and ethyl were not found to obstruct the dye aggregation, resulting in the downfall in efficiency using these spacers.

Thienoindoles have proved to have the potential to function both as donor as well as π-spacer units. Systematic engineering of different π-spacers and auxiliary donors to this moiety could bring impressive PCE in the future. In this line, dye designs that incorporate a TI unit with other indole fused systems open promising alternatives.

VI. Indolo[3,2-*b*]indole based sensitizers for DSSCs

Indolo[3,2-*b*]indoles[70] (IID) which consists of a central pyrrolo-pyrrole ring fused with two benzene rings on both sides, are considered as good electron donors with impressive hole-transporting properties. The planar nature of IID with a C_{2h}

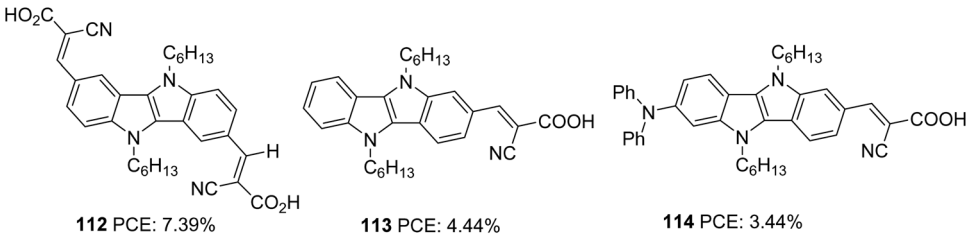

Fig. 36 Molecular structures of photosensitizers **112–114** with indolo[3,2-*b*]indole as a component.

symmetry facilitates better intermolecular interactions, which are beneficial for improving the hole transporting properties of these systems in the solid-state. In addition to these advantages, the two alkylation sites also make IID a potential candidate in various solution-processable optoelectronic applications such as organic thin film transistors, heterojunction solar cells, and organic light-emitting diodes.[71]

The first attempt to incorporate IID as a building block in a DSSC was carried out by Ruangsupapichat *et al.* (Fig. 36).[72] They developed dyes that fall in three categories: double acceptor system (**112**), donor–acceptor system (**113**), and donor–π spacer–acceptor (**114**). While IID functions as a donor in **112** and **113**, it assumes the linker function in **114**. The additional acceptor group and donor moieties in **112** and **114** helped to redshift the absorption spectra of the compounds by 30 nm and 10 nm, respectively with respect to **113**. The PCE of the dyes was in the range 3–7%. The difference in PCE of the dyes resulted from the difference in J_{sc} values. The highest J_{sc} of 14.56 mA cm^{-2} of **112** contributed towards achieving the highest efficiency of 7.39%. This resulted from the extra electron extraction pathways provided by the additional electron anchoring groups present in the molecule. The device fabricated with dye **114**, having an additional diphenylamine donor group, showcased the minor performance with only 3.44% PCE. According to the DFT studies, HOMO and LUMO energy levels of dye **114** are primarily localized on diphenylamine donors and cyanoacetic acid. Whereas in **112**, a good overlap of the HOMO and LUMO levels may favour effective electron injection to the semiconductor's conduction band. Less effective electron injection in **114** maybe lowering the J_{sc} (8.25 mA cm^{-2}) and thus the efficiency of the device (Table 6).

The same group further attempted to improve the efficiency of A–D–A dye **99** by introducing extra donor methoxyphenyl (**115**) and hexyloxyphenyl (**116**) moieties at the *N*,*N*′-positions of the IID core (Fig. 37).[73] The dyes show involvement of both the carboxyl groups on anchoring but differ significantly in their performance. Dye **116** outperformed **112** and **115** in J_{sc} (17.04 mA cm^{-2}) and V_{oc} (718 mV) values leading to a higher PCE of 7.86%. Dye **115** exhibited 5.20% PCE with J_{sc} of 11.59 mA cm^{-2} and V_{oc} of 638 mV. While the introduction of a longer alkyl chain in **116** was found to minimise recombination effectively, it also helped to improve the homogeneity of dye adsorption on the semiconductor surface. Broader absorption and higher dye loading amount improved the current density for **116**.

Our group also tried to explore the potential of IID as a donor unit towards the development of D–π–A dyes by introducing an additional π-spacer between the IID donor and cyanoacrylic acid acceptor and also by varying π-linkers between benzene, thiophene and furan (Fig. 38, **117**, **118**, **119**).[74] The donor unit IID was synthesized utilizing the methodology we developed in our laboratory, which involves a sequential multicomponent and oxidation approach.[75] The absorption spectra of **119** showed more red-shifted and intensified spectra followed by **118** and **117** in order. Nevertheless, the current density and V_{oc} produced by the compounds follow the reverse trend. To investigate the degree of conjugation, molecular geometry analysis of the dyes was also carried out. The acceptor group was found to be almost coplanar with the IID in all the dyes. But the dihedral angle between the donor and π-spacer increases in the order **119** (1.66°) < **118** (21.99°) < **117** (34.48°). Though the more planar geometry of **119** could help red shift the absorption spectra of the dye, it may also be entertaining

Table 6 Photovoltaic parameters of indolo[3,2-*b*]indole based DSSCs

Sensitizer	J_{sc} (mA cm^{-2})	V_{oc} (mV)	FF	PCE (%)	Electrolyte	Coadsorbent (concentration)	Ref.
112	14.56	740	0.68	7.39	I^-/I_3^-	—	72
113	10.09	660	0.66	4.44	I^-/I_3^-	—	72
114	8.25	620	0.68	3.44	I^-/I_3^-	—	72
115	11.59	638	0.70	5.20	I^-/I_3^-	—	73
116	17.04	718	0.64	7.86	I^-/I_3^-	—	73
117	5.51	620	0.69	2.38	I^-/I_3^-	CDCA (20 mM)	74
118	5.22	570	0.67	2.00	I^-/I_3^-	CDCA (20 mM)	74
119	4.60	540	0.69	1.71	I^-/I_3^-	CDCA (20 mM)	74
120	14.55	671	0.69	6.73	I^-/I_3^-	—	76
121	14.83	672	0.71	7.03	I^-/I_3^-	—	76
122	16.65	691	0.69	8.00	I^-/I_3^-	—	76
123	16.74	705	0.70	8.32	I^-/I_3^-	—	76

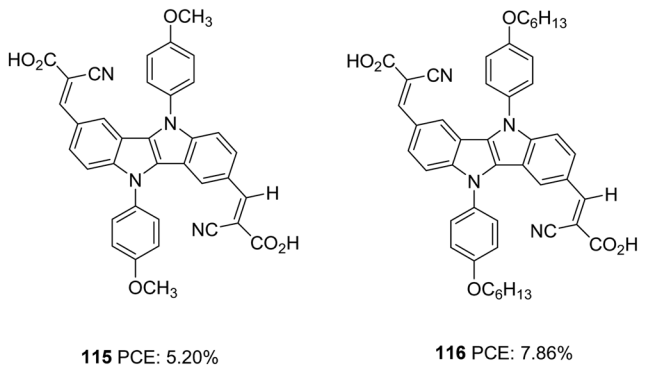

Fig. 37 Molecular structures of photosensitizers **115–116** with indolo[3,2-*b*]indole as the donor.

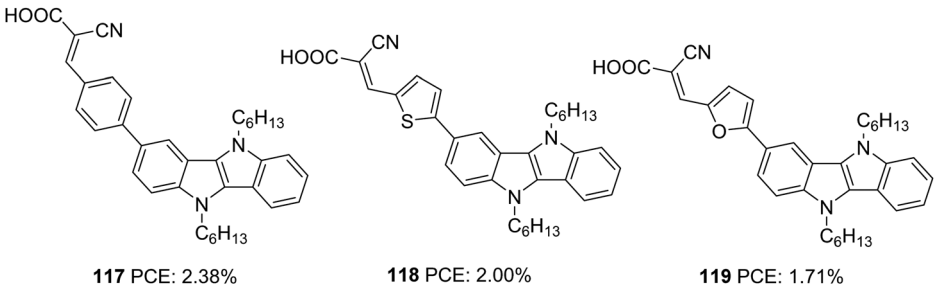

Fig. 38 Molecular structures of photosensitizers **117–119** with indolo[3,2-*b*]indole as the donor.

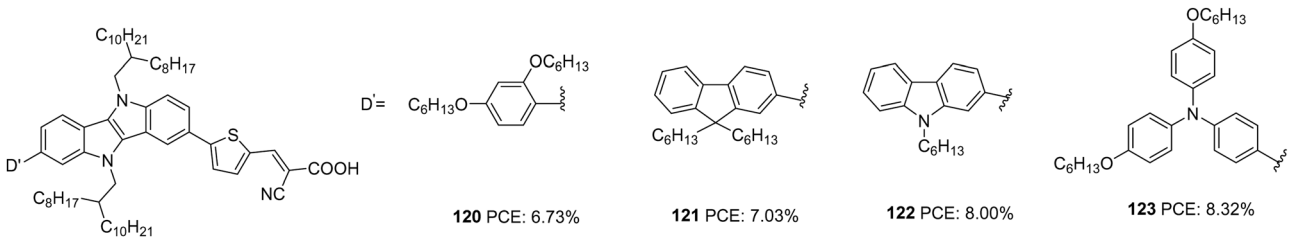

Fig. 39 Molecular structures of photosensitizers **120–123** with indolo[3,2-*b*]indole as the donor.

the aggregation between dye molecules, which could eventually lead to more recombination. A slightly twisted conformation of the benzene substituted dye could prevent the approach of oxidized species from the electrolyte to come close to the semiconductor and the formation of π-stacks, thereby decreasing the chance of recombination. The addition of CDCA enhanced the PCE in all the cases. To utilize the different absorption profile showcased by **119** where recombination destroyed the PCE, we custom designed BID dyes which will be discussed in detail in the next section.

Wang *et al.* synthesized four D–D–π–A dyes based on IID as the primary donor, thiophene as π-spacer and cyanoacrylic acid as an acceptor.[76] Dyes **120–123** contain hexyloxyphenyl, fluorene, carbazole and hexyloxytriphenylamine, respectively, as the auxiliary donor (Fig. 39). The current density and open-circuit potential followed the same trend, following the electron-donating ability and steric hindrance of the auxiliary donors. The bulkier and more electron-donating triphenylamine made **123** outperform other dyes with PCE of 8.32% with the highest J_{sc} of 16.74 mA cm^{-2} and V_{oc} of 705 mV. Other dyes exhibited efficiency in the order **122** > **121** > **120** (Table 6).

VII. Benzothieno[3,2-*b*]indole based sensitizers for DSSCs

Benzothieno[3,2-*b*]indole (BID) is another unique tetracene with a benzothiophene moiety fused to indole. This heteroacene has found applications in medicinal chemistry but is seldom used in materials science and optoelectronic applications.[77–79] Like what we discussed for indolo[3,2-*b*]indole; this fused indole moiety is also a planar conjugated system with the potential to be used both as a donor and a π-spacer. In addition, the appropriate functionalization of the N-atom offers flexibility to engineer the BID core with features that render better solubility and will also prevent aggregation of the system, arresting recombination.

As a continuation to our previous studies with indolo[3,2-*b*]-indole, the donor group was changed to dodecyl chain functionalized benzothieno[3,2-*b*]indole. Here also the newly developed methodology was employed for the synthesis of the BID core. The devices developed based on dyes **124** (phenyl spacer), **125** (thiophene spacer) and **126** (furan spacer) were found to showcase their best efficiency in the absence of any co-adsorbent. The addition of CDCA as a co-adsorbent decreased the photovoltaic performances of the devices. This illustrates the role of longer alkyl chains (dodecyl) in reducing aggregation of dyes and preventing back electron transfer. Unlike our observation with indolo[3,2-*b*]indole based dyes, furan substituted dye **126** outperformed the other two sensitizers with 4.11% efficiency with the highest J_{sc} and V_{oc} (Table 7 and Fig. 40).[80]

VIII. Tetraindole based sensitizers for DSSCs

The synthesis of tetraindole was first reported in 2006, which involved a one-pot tetramerization of indolin-2-one mediated by phosphoryl chloride.[81] This polyacene has four indole units fused to cyclooctatetraene, which acts as a promising donor motif for solar cell applications. In addition, the unique structural characteristics of this saddle-shaped scaffold will also prevent self-assembly of the dyes on the semiconductor surface.

Tetraindole found a place in DSSCs through the work of Qian and co-workers.[82] The D–π–A dyes **127** and **128** use thiophene and bithiophene, respectively, as π-bridges (Fig. 41).

Table 7 Photovoltaic parameters of DSSCs **124–140**

Sensitizer	J_{sc} (mA cm^{-2})	V_{oc} (mV)	FF	PCE (%)	Electrolyte	Coadsorbent (concentration)	Ref.
124	2.86	590	0.69	1.16	I^-/I_3^-	—	79
125	6.51	652	0.73	3.10	I^-/I_3^-	—	79
126	8.38	671	0.73	4.11	I^-/I_3^-	—	79
127	12.1	750	0.64	5.79	I^-/I_3^-	—	81
128	13.0	762	0.65	6.46	I^-/I_3^-	—	81
129	14.0	725	0.68	6.90	I^-/I_3^-	—	82
130	13.5	680	0.67	6.15	I^-/I_3^-	—	82
131	10.5	650	0.65	4.43	I^-/I_3^-	—	82
132	14.2	753	0.71	7.59	I^-/I_3^-	—	82
133	13.0	640	0.72	5.99	I^-/I_3^-	—	82
134	12.6	652	0.70	5.75	I^-/I_3^-	CDCA (0.3 mM)	83
135	13.8	657	0.71	6.42	I^-/I_3^-	CDCA (0.3 mM)	83
136	8.98	643	0.70	4.05	I^-/I_3^-	CDCA (0.3 mM)	83
137	12.1	633	0.70	5.37	I^-/I_3^-	CDCA (0.3 mM)	83
138	2.19	700	0.59	1.09	I^-/I_3^-	—	84
139	12.56	780	0.62	6.04	I^-/I_3^-	—	84
140	3.92	680	0.53	1.42	I^-/I_3^-	—	84

The dyes exhibit improved open-circuit potential benefitting from the saddle like structure with flanked octyl alkyl chains of the new donor moiety. The sensitizer **128** exhibited a broader ICT band and better light-harvesting ability, which is evident from the broader and enhanced response of the IPCE spectra. **128** delivered a maximum efficiency of 6.21% with the highest J_{sc} (13.0 mA cm^{-2}) and V_{oc} (762 mV), whereas dye **127** could only deliver a PCE of 5.79% with J_{sc} of 12.1 mA cm^{-2} and V_{oc} of 750 mV. The reduced aggregation behaviour of these dye was further illustrated by the co-adsorption experiments using CDCA. Both dyes exhibited lower efficiencies in the presence of CDCA, the reduction mainly arose from lower J_{sc} values (Table 7). Decreased dye loading in the presence of CDCA can account for the decrease in photocurrent and hence the overall efficiency.

IX. Dithienopyrroloindole based sensitizers for DSSCs

Optimization of the π-bridge is also as important as other building blocks in a photosensitizer to realize improved PCE. Rigidified aromatics occupy a prominent space among various conjugated functionalities in this regard due to their better charge transfer ability, high molar extinction coefficient and reduced reorganization energies. The compound 4,5-dihexyl-4,5-dihydrothieno[2″,3″:4′,5′]pyrrolo[2′,3′:4,5]thieno[3,2-*b*]indole (DPTI) as a π-spacer was first employed by Zang *et al.* to construct photosensitizers **129**, **131–133** (Fig. 42).[83] To compare the efficiency of a dithienopyrroloindole (DTP) unit as a spacer, dye **130** was synthesized. Dye **129** outperformed **130** with improved light-harvesting ability and open-circuit potential, indicating the importance of DPTI over DTP. Dyes **131** and **132** were designed to investigate the effect of additional donor and alkylated spacer units on the performance of DPTI based dye. The introduction of an additional donor unit in **131** caused a negative shift in HOMO compared to **129**, whereas a positive shift in LUMO energy level was observed in **132** without much change in HOMO energy level. This low driving force for dye regeneration, enhanced recombination of electrons from the semiconductor with the oxidized dye and lowest dye loading may be responsible for the least efficiency of 4.4% for **131**. The broader spectra of **132** with its twisted conformation induced by the 3-hexylthiophene could deliver a maximum efficiency of 7.59%. In dye **133**, the DPTI unit assumes both the function of a donor and spacer, the indole ring acting as the donor and DTP as the spacer. The conjugated donor–π-spacer structure allows better delocalization of the HOMO and LUMO orbitals over the entire molecule and facilitates good charge transfer from donor to acceptor. Though it managed to perform better than **131**, the lack of additional donor decreased the charge

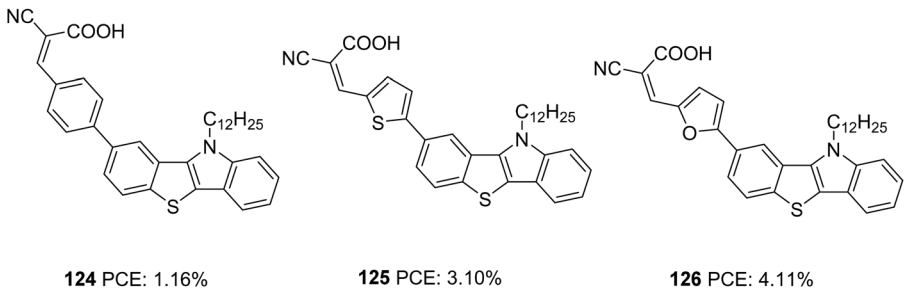

124 PCE: 1.16% **125** PCE: 3.10% **126** PCE: 4.11%

Fig. 40 Molecular structures of photosensitizers **124–126** with benzothieno[3,2-*b*]indole as the donor.

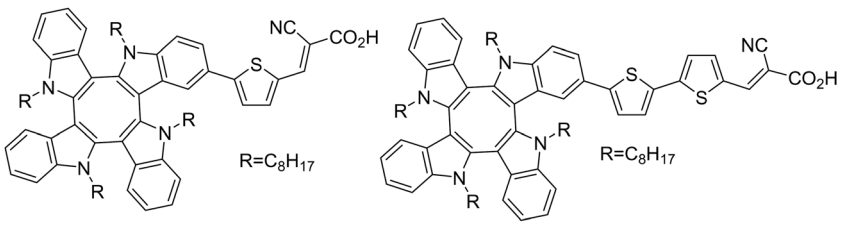

127 PCE: 5.79% **128** PCE: 6.46%

Fig. 41 Photosensitizers **127–128** with tetraindole as the donor.

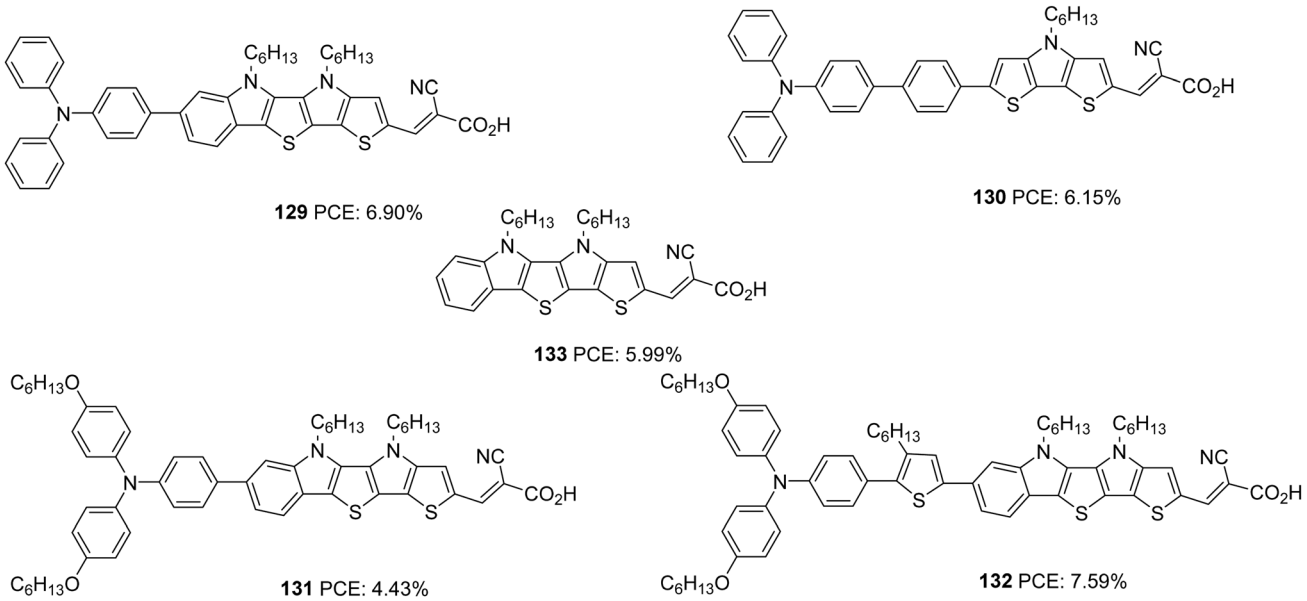

Fig. 42 Molecular structure of photosensitizers **129–133** with dithienopyrroloindole as a component.

separation and electron injection yield leading to lower photocurrent and an efficiency of 5.99%, lower than the rest of the dyes.

X. Fluorenylindolenine donor-based dyes for DSSCs

Jayaraj and co-workers synthesized four novel unsymmetrical squaraine dyes employing fluorenylindolenine as donor **134–137** (Fig. 43).[84] Apart from increasing the conjugation and NIR light-harvesting capability of the molecules, this skeleton also helps to modulate the charge recombination by incorporating an out of plane alkyl chain on sp^3 carbon and in-plane alkyl chain on the nitrogen. While **134** and **135** are composed of an indole unit toward the anchoring side with an *N*-methylated and *N*-hexylated fluorenylindolenine, **136** and **137** contained a benzo[*e*]indole unit toward the anchoring side with an *N*-methylated and *N*-hexylated donor, respectively. Though the latter set showcased more red-shifted spectra, they exhibited slightly lower efficiency. The difference in PCE of the devices might be due to the difference in dipole moment of the dyes. The calculated dipole moments are in the order **135** (10.6) > **134** (10.0 D) > **136** (7.4 D) > **137** (7.3 D). The non-directionality induced by the benz[*e*]indole group in **136–137** may be responsible for lowering the dipole moment and electron injection efficiency. The larger dipole moment exerted by dyes **134–135** on TiO_2 may also be helping to upshift the conduction band of TiO_2, which is evident from the higher V_{oc} observed for these dyes. In both sets of dyes, the hexyl substituted dyes were found to outperform the methylated dye. All the dyes exhibited an increment in PCE when dye and CDCA were used in 1:3 ratios, the effect majorly contributed by the increase in current density. It is already known that squaraines are prone to aggregation. Adding CDCA helps to reduce this aggregation leading to improved PCE.

XI. Indole–imidazole donor dyes for DSSC

An indole–imidazole fused system was incorporated as an auxiliary acceptor (AN) by Ramasami to construct three dyes with different molecular architectures: **138** (D–AN(π–A)–D), **139**

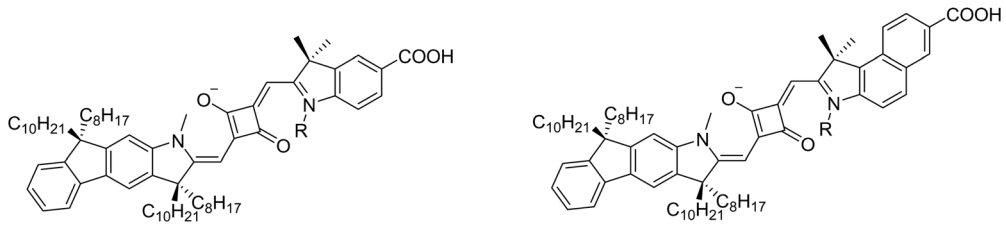

Fig. 43 Molecular structure of photosensitizers **134–137** with fluorenylindolenine as the donor.

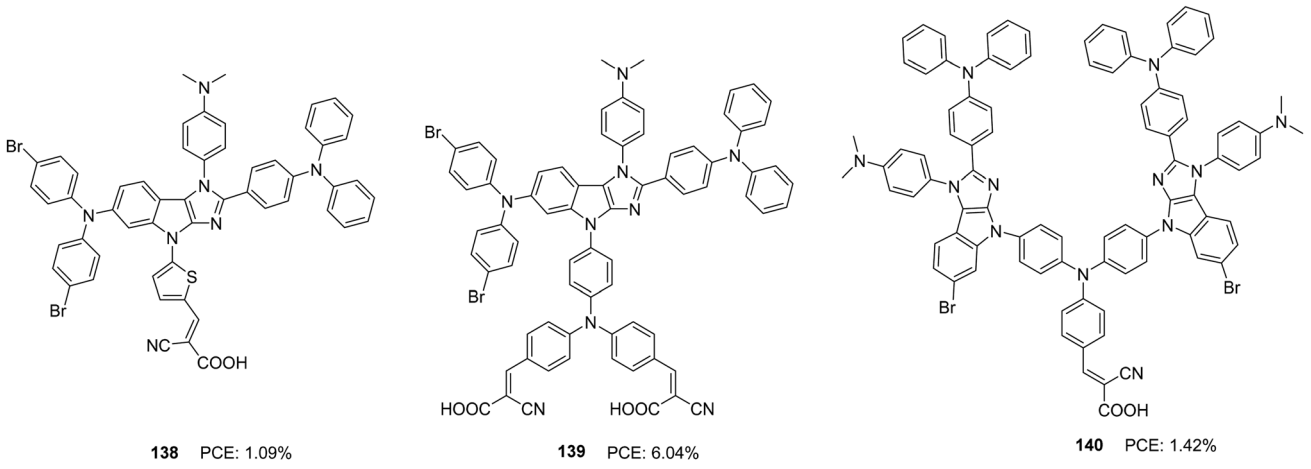

138 PCE: 1.09% **139** PCE: 6.04% **140** PCE: 1.42%

Fig. 44 Molecular structure of photosensitizers **138–140** imidazoloindole as the donor.

(D–AN–(DA_2)–D) and **140** (D–AN–D(A)–AN–D) (Fig. 44).[85] Dye **139** showed maximum efficiency with the highest current density and photovoltage. Along with the increment in molar extinction coefficient and red-shifted absorption, the dianchoring approach also facilitated adequate surface coverage and helped to reduce back electron transfer between the semiconductor surface and electrolyte. The minimum reorganization energy calculated for the same also implies efficient charge injection to the semiconductor for these dyes. The photovoltaic parameters of DSSCs **124–140** are given in Table 7.

Conclusions and future perspectives

Engineering sensitizers have got their prime importance when efficiency enhancement of DSSCs is concerned. Electron rich fused heterocycles have proved their efficacy as donors as well as π-spacers in the sensitizer design. Indole fused aromatic systems have also been utilized to this end, effectively realizing efficient DSSCs. These systems were found to exhibit more electron-donating ability than indole in conjugation with expanded π-systems. Though the planarity could induce ICT in molecules, a trade-off between light harvesting and dye aggregations leads to a shortfall of the power conversion efficiency in many instances. The strategic introduction of bulky substituents on the donor side and the π-conjugator helped abate these situations to some extent. Another notable advantage is the ease of synthesising fused indole heterocyclic motifs with functionalities required for further transformations. In addition, the stability of these fused heterocycles has contributed to enhancing the device lifetime.

The most efficient DSSC (PCE: 13.6%) with a fused indole based sensitizer was reported with dye **68**, which had a triazatruxene moiety as a donor unit. There are still a plethora of easily accessible fused indole heterocyclic moieties with the required structural features that can act as suitable donors and π-spacers in sensitizer designs. One of the simplest fused indole heteroacenes used as a sensitizer building block is thieno[3,2-*b*]indole, which gave DSSCs up to 11% efficiency. Likewise, pyrrolo[3,2-*b*]indole can be utilized, resulting in high performing DSSCs. The class of indole fused tetraacenes such as indoloindoles, benzothienoindoles and benzofuroindoles, which are excellent donors, are seldom used building blocks in sensitizer designs. These tetraacenes can exist as different isomers based on the position of fusion, and these isomers differ in their structure and properties and these have all the structural and electronic characteristics to act as good π-spacers. Moreover, these heteroacenes can be used in alternate and new sensitizer designs such as D–A–π–A or $(D)_2$–A–π–A, resulting in highly efficient DSSCs. As part of our continued interest in this area, we focus on developing new and simpler methodologies to access indole fused heterocycles and extend our research detailed in Section VI and VII by incorporating additional donors and auxiliary acceptors to the D–π–A architecture being optimized.

The challenging task in realizing efficient DSSCs is to prevent back electron transfer/recombination. Along with the proper molecular design and keeping a delicate balance between electronic and steric factors, importance must also be given to the electrolyte used. Significant improvement in photovoltaic parameters and the devices' performance is reported for **98** to **102** when the electrolyte was changed from I^-/I_3^- to $[Co(bpy)_3]^{2+/3+}$. Most of the sensitizers mentioned in the review use conventional iodide/triiodide electrolyte. This indicates that more promising results could be obtained in the future using appropriate alternate cobalt and copper electrolytes with these fused heterocyclic dyes. In addition, these fused heterocycles can serve as excellent co-sensitizers along with other dyes tapping the visible absorption for indoor photovoltaic applications. With continuing efforts to develop stable, easily accessible and efficient sensitizers for DSSCs, we hope significant advancements will be made with fused indole heterocyclic moieties in the near future.

Conflicts of interest

There are no conflicts of interest to declare.

Acknowledgements

The authors thank DST for DST-SERB Project [DST/SERB/F/481]. NPR thanks CSIR for the research fellowship. NPR and JJ also thanks CSIR (HCP-029) for financial assistance. SS would like to thank SERB CRG project (CRG/2020/001406) and CSIR-FIRST (MLP65) project. SS also acknowledges CSIR Mission (HCP30) and FTT (MLP38) Projects for financial support.

References

1 X. Chen, C. Li, M. Grätzel, R. Kostecki and S. S. Mao, Nanomaterials for renewable energy production and storage, *Chem. Soc. Rev.*, 2012, **41**, 7909–7937.

2 (*a*) N. Armaroli and V. Balzani, The future of energy supply: Challenges and opportunities, *Angew. Chem., Int. Ed.*, 2007, **46**, 52–66; (*b*) R. Eisenberg and D. G. Nocera, Preface: Overview of the forum on solar and renewable energy, *Inorg. Chem.*, 2005, **44**, 6799–6801.

3 (*a*) W. A. Badawy, A review on solar cells from Si-single crystals to porous materials and quantum dots, *J. Adv. Res.*, 2015, **6**, 123–132; (*b*) S. Sharma, K. K. Jain and A. Sharma, Solar cells: In research and applications—a review, *Mater. Sci. Appl.*, 2015, **06**, 1145–1155.

4 (*a*) M. Grätzel, Solar energy conversion by dye-sensitized photovoltaic cells, *Inorg. Chem.*, 2005, **44**, 6841–6851; (*b*) I. Chung, B. Lee, J. He, R. P. H. Chang and M. G. Kanatzidis, All-solid-state dye-sensitized solar cells with high efficiency, *Nature*, 2012, **485**, 486–489; (*c*) Y. Huang, E. J. Kramer, A. J. Heeger and G. C. Bazan, Bulk heterojunction solar cells: Morphology and performance relationships, *Chem. Rev.*, 2014, **114**, 7006–7043; (*d*) I. Mora-Seró, Current challenges in the development of quantum dot sensitized solar cells, *Adv. Energy Mater.*, 2020, **10**, 1–6; (*e*) O. E. Semonin, J. M. Luther and M. C. Beard, Quantum dots for next-generation photovoltaics, *Mater. Today*, 2012, **15**, 508–515; (*f*) M. A. Green, A. Ho-Baillie and H. J. Snaith, The emergence of perovskite solar cells, *Nat. Photonics*, 2014, **8**, 506–514; (*g*) R. Rajeswari, M. Mrinalini, S. Prasanthkumar and L. Giribabu, Emerging of inorganic hole transporting materials for perovskite solar cells, *Chem. Rec.*, 2017, **17**, 681–699.

5 G. Gokul, S. C. Pradhan and S. Soman, Dye sensitized solar cells as potential candidates for indoor/diffused light harvesting applications: From BIPV to self powered IoTs, *Adv. Sol. Energy Res.*, 2019, 281–316.

6 B. O'Regan and M. Grätzel, A low-cost, high-efficiency solar cell based on dye-sensitized colloidal TiO_2 films, *Nature*, 1991, **353**, 737–740.

7 (*a*) J. Gong, J. Liang and K. Sumathy, Review on dye-sensitized solar cells (DSSCs): Fundamental concepts and novel materials, *Renewable Sustainable Energy Rev.*, 2012, **16**, 5848–5860; (*b*) Z. Ning, Y. Fu and H. Tian, Improvement of dye-sensitized solar cells: What we know and what we need to know, *Energy Environ. Sci.*, 2010, **3**, 1170–1181; (*c*) T. Bessho, S. M. Zakeeruddin, C. Y. Yeh, E. W. G. Diau and M. Grätzel, Highly efficient mesoscopic dye-sensitized solar cells based on donor-acceptor-substituted porphyrins, *Angew. Chem., Int. Ed.*, 2010, **49**, 6646–6649; (*d*) A. Hagfeldt, G. Boschloo, L. Sun, L. Kloo and H. Pettersson, Dye-sensitized solar cells, *Chem. Rev.*, 2010, **110**, 6595–6663; (*e*) H. S. Jung and J. K. Lee, Dye sensitized solar cells for economically viable photovoltaic systems, *J. Phys. Chem. Lett.*, 2013, **4**, 1682–1693.

8 (*a*) H. Michaels, M. Rinderle, R. Freitag, I. Benesperi, T. Edvinsson, R. Socher, A. Gagliardi and M. Freitag, Dye-sensitized solar cells under ambient light powering machine learning: Towards autonomous smart sensors for the internet of things, *Chem. Sci.*, 2020, **11**, 2895–2906; (*b*) E. Tanaka, H. Michaels, M. Freitag and N. Robertson, Synergy of co-sensitizers in a copper bipyridyl redox system for efficient and cost-effective dye-sensitized solar cells in solar and ambient light, *J. Mater. Chem. A*, 2020, **8**, 1279–1287; (*c*) Y. Cao, Y. Liu, S. M. Zakeeruddin, A. Hagfeldt and M. Grätzel, *Joule*, 2018, **2**, 1108–1117; (*d*) S. Sasidharan, S. Soman, S. C. Pradhan, K. N. N. Unni, A. A. P. Mohamed, B. N. Nair and H. U. N. Saraswathy, *New J. Chem.*, 2017, **41**, 1007–1016; (*e*) M. Freitag, J. Teuscher, Y. Saygili, X. Zhang, F. Giordano, P. Liska, J. Hua, S. M. Zakeeruddin, J. E. Moser, M. Grätzel and A. Hagfeldt, Dye-sensitized solar cells for efficient power generation under ambient lighting, *Nat. Photonics*, 2017, **11**, 372–378; (*f*) S. Venkatesan, W. H. Lin, H. Teng and Y. L. Lee, High-efficiency bifacial dye-sensitized solar cells for application under indoor light conditions, *ACS Appl. Mater. Interfaces*, 2019, **11**, 42780–42789.

9 (*a*) J. M. Ji, H. Zhou and H. K. Kim, Rational design criteria for D–π–A structured organic and porphyrin sensitizers for highly efficient dye-sensitized solar cells, *J. Mater. Chem. A*, 2018, **6**(30), 14518–14545; (*b*) W. Wei, K. Sun and Y. H. Hu, An efficient counter electrode material for dye-sensitized solar cells – flower-structured 1T metallic phase MoS2, *J. Mater. Chem. A*, 2016, **4**(32), 12398–12401; (*c*) W. Wei, K. Sun and Y. H. Hu, Direct conversion of CO2 to 3D graphene and its excellent performance for dye-sensitized solar cells with 10% efficiency, *J. Mater. Chem. A*, 2016, **4**(31), 12054–12057; (*d*) D. Wang, W. Wei and Y. H. Hu, Highly efficient dye-sensitized solar cells with composited food dyes, *Ind. Eng. Chem. Res.*, 2020, **59**(22), 10457–10463.

10 (*a*) Q. Huaulmé, V. M. Mwalukuku, D. Joly, J. Liotier, Y. Kervella, P. Maldivi, S. Narbey, F. Oswald, A. J. Riquelme, J. A. Anta and R. Demadrille, Photochromic dye-sensitized solar cells with light-driven adjustable optical transmission and power conversion efficiency, *Nat. Energy*, 2020, **5**, 468–477; (*b*) A. Gopi, S. Lingamoorthy, S. Soman, K. Yoosaf, R. Haridas and S. Das, Modulating FRET in organic–inorganic nanohybrids for light harvesting applications, *J. Phys. Chem. C*, 2016, **120**, 26569–26578; (*c*) M. V. Vinayak, M. Yoosuf, S. C. Pradhan, T. M. Lakshmykanth, S. Soman and K. R. Gopidas, A detailed evaluation of charge recombination dynamics in dye solar cells based on starburst triphenylamine dyes, *Sustainable Energy Fuels*, 2018, **2**, 303–314; (*d*) H. Iftikhar, G. G. Sonai, S. G. Hashmi, A. F. Nogueira and P. D. Lund, Progress on electrolytes development in dye-sensitized solar

cells, *Materials*, 2019, **12**, 1998–2065; (*e*) S. C. Pradhan, A. Hagfeldt and S. Soman, Resurgence of DSCs with copper electrolyte: a detailed investigation of interfacial charge dynamics with cobalt and iodine based electrolytes, *J. Mater. Chem. A*, 2018, **6**, 22204–22214; (*f*) S. Soman, Y. Xie and T. W. Hamann, Cyclometalated sensitizers for DSSCs employing cobalt redox shuttles, *Polyhedron*, 2014, **82**, 139–147; (*g*) S. Soman, M. A. Rahim, S. Lingamoorthy, C. H. Suresh and S. Das, Strategies for optimizing the performance of carbazole thiophene appended unsymmetrical squaraine dyes for dye-sensitized solar cells, *Phys. Chem. Chem. Phys.*, 2015, **17**, 23095–23103; (*h*) M. V. Vinayak, T. M. Lakshmykanth, M. Yoosuf, S. Soman and K. R. Gopidas, Effect of recombination and binding properties on the performance of dye sensitized solar cells based on propeller shaped triphenylamine dyes with multiple binding groups, *Sol. Energy*, 2016, **124**, 227–241; (*i*) Q. Wali, A. Fakharuddin and R. Jose, Tin oxide as a photoanode for dye-sensitised solar cells: Current progress and future challenges, *J. Power Sources*, 2015, **293**, 1039–1052.

11 (*a*) K. L. Wu, W. P. Ku, J. N. Clifford, E. Palomares, S. Te Ho, Y. Chi, S. H. Liu, P. T. Chou, M. K. Nazeeruddin and M. Grätzel, Harnessing the open-circuit voltage *via* a new series of Ru(II) sensitizers bearing (iso-)quinolinyl pyrazolate ancillaries, *Energy Environ. Sci.*, 2013, **6**, 859–870; (*b*) Z. She, Y. Cheng, L. Zhang, X. Li, D. Wu, Q. Guo, J. Lan, R. Wang and J. You, Novel ruthenium sensitizers with a phenothiazine conjugated bipyridyl ligand for high-efficiency dye-sensitized solar cells, *ACS Appl. Mater. Interfaces*, 2015, **7**, 27831–27837; (*c*) L. Han, A. Islam, H. Chen, C. Malapaka, B. Chiranjeevi, S. Zhang, X. Yang and M. Yanagida, High-efficiency dye-sensitized solar cell with a novel co-adsorbent, *Energy Environ. Sci.*, 2012, **5**, 6057–6060.

12 (*a*) Y. S. Yen, H. H. Chou, Y. C. Chen, C. Y. Hsu and J. T. Lin, Recent developments in molecule-based organic materials for dye-sensitized solar cells, *J. Mater. Chem.*, 2012, **22**, 8734–8747; (*b*) A. Mishra, M. K. R. Fischer and P. Büuerle, Metal-free organic dyes for dye-sensitized solar cells: From structure: Property relationships to design rules, *Angew. Chem., Int. Ed.*, 2009, **48**, 2474–2499; (*c*) A. Carella, F. Borbone and R. Centore, Research progress on photosensitizers for DSSC, *Front. Chem.*, 2018, **6**, 1–24.

13 (*a*) J. J. Cid, J. H. Yum, S. R. Jang, M. K. Nazeeruddin, E. Martínez-Ferrero, E. Palomares, J. Ko, M. Grätzel and T. Torres, Molecular cosensitization for efficient panchromatic dye-sensitized solar cells, *Angew. Chem., Int. Ed.*, 2007, **46**, 8358–8362; (*b*) N. V. Krishna, J. V. S. Krishna, M. Mrinalini, S. Prasanthkumar and L. Giribabu, Role of co-sensitizers in dye-sensitized solar cells, *ChemSusChem*, 2017, **10**, 4668–4689.

14 (*a*) B. Hemavathi, V. Jayadev, P. C. Ramamurthy, R. K. Pai, K. N. Narayanan Unni, T. N. Ahipa, S. Soman and R. G. Balakrishna, Variation of the donor and acceptor in D–A–π–A based cyanopyridine dyes and its effect on dye sensitized solar cells, *New J. Chem.*, 2019, **43**, 15673–15680; (*b*) B. Hemavathi, V. Jayadev, S. C. Pradhan, G. Gokul, K. Jagadish, G. K. Chandrashekara, P. C. Ramamurthy, R. K. Pai, K. N. Narayanan Unni, T. N. Ahipa, S. Soman and R. Geetha Balakrishna, Aggregation induced light harvesting of molecularly engineered D–A–π–A carbazole dyes for dye-sensitized solar cells, *Sol. Energy*, 2018, **174**, 1085–1096; (*c*) T. Maeda, T. V. Nguyen, Y. Kuwano, X. Chen, K. Miyanaga, H. Nakazumi, S. Yagi, S. Soman and A. Ajayaghosh, Intramolecular exciton-coupled squaraine dyes for dye-sensitized solar cells, *J. Phys. Chem. C*, 2018, **122**, 21745–21754; (*d*) V. Nikolaou, A. Charisiadis, S. Chalkiadaki, I. Alexandropoulos, S. C. Pradhan, S. Soman, M. K. Panda and A. G. Coutsolelos, Enhancement of the photovoltaic performance in D3A porphyrin-based DSCs by incorporating an electron withdrawing triazole spacer, *Polyhedron*, 2018, **140**, 9–18; (*e*) J. S. Panicker, B. Balan, S. Soman and V. C. Nair, Understanding structure–property correlation of metal free organic dyes using interfacial electron transfer measurements, *Sol. Energy*, 2016, **139**, 547–556; (*f*) S. Soman, S. C. Pradhan, M. Yoosuf, M. V. Vinayak, S. Lingamoorthy and K. R. Gopidas, Probing recombination mechanism and realization of marcus normal region behavior in DSSCs employing cobalt electrolytes and triphenylamine dyes, *J. Phys. Chem. C*, 2018, **122**, 14113–14127; (*g*) M. Yoosuf, S. C. Pradhan, S. Soman and K. R. Gopidas, Triple bond rigidified anthracene–triphenylamine sensitizers for dye-sensitized solar cells, *Sol. Energy*, 2019, **188**, 55–65.

15 (*a*) L. Zhang, X. Yang, W. Wang, G. G. Gurzadyan, J. Li, X. Li, J. An, Z. Yu, H. Wang, B. Cai, A. Hagfeldt and L. Sun, 13.6% Efficient organic dye-sensitized solar cells by minimizing energy losses of the excited state, *ACS Energy Lett.*, 2019, **4**, 943–951; (*b*) W. Zhang, Y. Wu, H. W. Bahng, Y. Cao, C. Yi, Y. Saygili, J. Luo, Y. Liu, L. Kavan, J. E. Moser, A. Hagfeldt, H. Tian, S. M. Zakeeruddin, W. H. Zhu and M. Grätzel, Comprehensive control of voltage loss enables 11.7% efficient solid-state dye-sensitized solar cells, *Energy Environ. Sci.*, 2018, **11**, 1779–1787; (*c*) Y. Cao, Y. Liu, S. M. Zakeeruddin, A. Hagfeldt and M. Gratzel, Direct contact of selective charge extraction layers enables high-efficiency molecular photovoltaics, *Joule*, 2018, **2**, 1108–1117; (*d*) K. Kakiage, Y. Aoyama, T. Yano, K. Oya, J. Fujisawa and M. Hanaya, Highly-efficient dye-sensitized solar cells with collaborative sensitization by silyl-anchor and carboxy-anchor dyes, *Chem. Commun.*, 2015, **51**, 15894–15897.

16 (*a*) L. Alibabaei, J. H. Kim, M. Wang, N. Pootrakulchote, J. Teuscher, D. Di Censo, R. Humphry-Baker, J. E. Moser, Y. J. Yu, K. Y. Kay, S. M. Zakeeruddin and M. Grätzel, Molecular design of metal-free D–π–A substituted sensitizers for dye-sensitized solar cells, *Energy Environ. Sci.*, 2010, **3**, 1757–1764; (*b*) A. Yella, R. Humphry-Baker, B. F. E. Curchod, N. Ashari Astani, J. Teuscher, L. E. Polander, S. Mathew, J. E. Moser, I. Tavernelli, U. Rothlisberger, M. Grätzel, M. K. Nazeeruddin and J. Frey, Molecular engineering of a fluorene donor for dye-sensitized solar cells, *Chem. Mater.*, 2013, **25**, 2733–2739.

17 (*a*) J. Wang, K. Liu, L. Ma and X. Zhan, Triarylamine: Versatile platform for organic, dye-sensitized, and perovskite solar cells,

Chem. Rev., 2016, **116**, 14675–14725; (*b*) K. Hara, K. Sayama, Y. Ohga, A. Shinpo, S. Suga and H. Arakawa, A coumarin-derivative dye sensitized nanocrystalline TiO2 solar cell having a high solar-energy conversion efficiency up to 5.6%, *Chem. Commun.*, 2001, 569–570; (*c*) Z. S. Wang, K. Hara, Y. Dan-oh, C. Kasada, A. Shinpo, S. Suga, H. Arakawa and H. Suglhara, Photophysical and (photo)electrochemical properties of a coumarin dye, *J. Phys. Chem. B*, 2005, **109**, 3907–3914; (*d*) B. Liu, R. Wang, W. Mi, X. Li and H. Yu, Novel branched coumarin dyes for dye-sensitized solar cells: Significant improvement in photovoltaic performance by simple structure modification, *J. Mater. Chem.*, 2012, **22**, 15379–15387; (*e*) M. Marszalek, S. Nagane, A. Ichake, R. Humphry-Baker, V. Paul, S. M. Zakeeruddin and M. Grätzel, Tuning spectral properties of phenothiazine based donor-π-acceptor dyes for efficient dye-sensitized solar cells, *J. Mater. Chem.*, 2012, **22**, 889–894; (*f*) S. H. Kim, H. W. Kim, C. Sakong, J. Namgoong, S. W. Park, M. J. Ko, C. H. Lee, W. I. Lee and J. P. Kim, Effect of five-membered heteroaromatic linkers to the performance of phenothiazine-based dye-sensitized solar cells, *Org. Lett.*, 2011, **13**, 5784–5787; (*g*) K. Srinivas, C. R. Kumar, M. A. Reddy, K. Bhanuprakash, V. J. Rao and L. Giribabu, D–π–A organic dyes with carbazole as donor for dye-sensitized solar cells, *Synth. Met.*, 2011, **161**, 96–105.

18 (*a*) Y. Liu, J. He, L. Han and J. Gao, Influence of the auxiliary acceptor and π-bridge in carbazole dyes on photovoltaic properties, *J. Photochem. Photobiol., A*, 2017, **332**, 283–292; (*b*) K. Hara, Z. S. Wang, T. Sato, A. Furube, R. Katoh, H. Sugihara, Y. Dan-Oh, C. Kasada, A. Shinpo and S. Suga, Oligothiophene-containing coumarin dyes for efficient dye-sensitized solar cells, *J. Phys. Chem. B*, 2005, **109**, 15476–15482; (*c*) J. Liu, X. Yang, A. Islam, Y. Numata, S. Zhang, N. T. Salim, H. Chen and L. Han, Efficient metal-free sensitizers bearing circle chain embracing π-spacers for dye-sensitized solar cells, *J. Mater. Chem. A*, 2013, **1**, 10889–10897; (*d*) L. Huang, P. Ma, G. Deng, K. Zhang, T. Ou, Y. Lin and M. S. Wong, Novel electron-deficient quinoxaline-dithienothiophene- and phenazinedithienothiophene-based photosensitizers: The effect of conjugation expansion on DSSC performance, *Dyes Pigm.*, 2018, **159**, 107–114.

19 (*a*) Y. Wu and W. Zhu, Organic sensitizers from D–π–A to D–A–π–A: Effect of the internal electron-withdrawing units on molecular absorption, energy levels and photovoltaic performances, *Chem. Soc. Rev.*, 2013, **42**, 2039–2058; (*b*) W. Zhu, Y. Wu, S. Wang, W. Li, X. Li, J. Chen, Z. S. Wang and H. Tian, Organic D–A–π–A solar cell sensitizers with improved stability and spectral response, *Adv. Funct. Mater.*, 2011, **21**, 756–763; (*c*) W. Li, Y. Wu, Q. Zhang, H. Tian and W. Zhu, D–A–π–A featured sensitizers bearing phthalimide and benzotriazole as auxiliary acceptor: Effect on absorption and charge recombination dynamics in dye-sensitized solar cells, *ACS Appl. Mater. Interfaces*, 2012, **4**, 1822–1830; (*d*) Y. Wu, W. H. Zhu, S. M. Zakeeruddin and M. Grätzel, Insight into D–A–π–A structured sensitizers: A promising route to highly efficient and stable dye-sensitized solar cells, *ACS Appl. Mater. Interfaces*, 2015, **7**, 9307–9318; (*e*) J. He, Y. Liu, J. Gao and L. Han, New D–D–π–A triphenylamine-coumarin sensitizers for dye-sensitized solar cells, *Photochem. Photobiol. Sci.*, 2017, **16**, 1049–1056; (*f*) W. Sharmoukh, J. Cong, J. Gao, P. Liu, Q. Daniel and L. Kloo, Molecular engineering of D–D–π–A-based organic sensitizers for enhanced dye-sensitized solar cell performance, *ACS Omega*, 2018, **3**, 3819–3829; (*g*) V. Cuesta, M. Vartanian, P. de la Cruz, R. Singhal, G. D. Sharma and F. Langa, Comparative study on the photovoltaic characteristics of A–D–A and D–A–D molecules based on Zn-porphyrin; a D–A–D molecule with over 8.0% efficiency, *J. Mater. Chem. A*, 2017, **5**, 1057–1065; (*h*) K. S. V. Gupta, T. Suresh, S. P. Singh, A. Islam, L. Han and M. Chandrasekharam, Carbazole based A–π–D–π–A dyes with double electron acceptor for dye-sensitized solar cell, *Org. Electron.*, 2014, **15**, 266–275.

20 (*a*) I. Cho, S. K. Park, B. Kang, J. W. Chung, J. H. Kim, K. Cho and S. Y. Park, Design, synthesis, and versatile processing of indolo[3,2-*b*]indole-based π-conjugated molecules for high-performance organic field-effect transistors, *Adv. Funct. Mater.*, 2016, **26**, 2966–2973; (*b*) Y. Y. Lai, J. M. Yeh, C. E. Tsai and Y. J. Cheng, Synthesis, molecular and photovoltaic properties of an indolo[3,2-*b*]indole-based acceptor–donor–acceptor small molecule, *Eur. J. Org. Chem.*, 2013, 5076–5084; (*c*) H. Jiang, H. Zhao, K. K. Zhang, X. Chen, C. Kloc and W. Hu, High-performance organic single-crystal field-effect transistors of indolo[3,2-*b*]carbazole and their potential applications in gas controlled organic memory devices, *Adv. Mater.*, 2011, **23**, 5075–5080.

21 For the synthesis of indolo[2,3-*b*]quinoxaline see: G. M. Badger and P. J. Nelson, Polynuclear heterocyclic systems. Part XIV. Indoloquinoxalines, *J. Chem. Soc.*, 1962, 3926–3931.

22 K. R. J. Thomas and P. Tyagi, Synthesis, Spectra, and Theoretical Investigations of the Triarylamines Based on 6H-Indolo[2,3-*b*]quinoxaline, *J. Org. Chem.*, 2010, **75**, 8100–8111.

23 A. Venkateswararao, P. Tyagi, K. R. J. Thomas and P. Chen, Organic dyes containing indolo [2, 3- b] quinoxaline as a donor: synthesis, optical and photovoltaic properties, *Tetrahedron*, 2014, **70**, 6318–6327.

24 X. Qian, H. H. Gao, Y. Z. Zhu, L. Lu and J. Y. Zheng, 6*H*-Indolo[2,3-*b*]quinoxaline-based organic dyes containing different electron-rich conjugated linkers for highly efficient dye-sensitized solar cells, *J. Power Sources*, 2015, **280**, 573–580.

25 X. Qian, X. Wang, L. Shao, H. Li, R. Yan and L. Hou, Molecular engineering of D–D–π–A type organic dyes incorporating indoloquinoxaline and phenothiazine for highly efficient dye-sensitized solar cells, *J. Power Sources*, 2016, **326**, 129–136.

26 X. Qian, X. Lan, R. Yan, Y. He, J. Huang and L. Hou, T-shaped (D)2–A–π–A type sensitizers incorporating indoloquinoxaline and triphenylamine for organic dye-sensitized solar cells, *Electrochim. Acta*, 2017, **232**, 377–386.

27 R. Su, L. Lyu, M. R. Elmorsy and A. El-Shafei, Novel metal-free organic dyes constructed with the D–D|A–π–A motif: Sensitization and co-sensitization study, *Sol. Energy*, 2019, **194**, 400–414.

28 R. Su, S. Ashraf, L. Lyu and A. El-shafei, Tailoring dual-channel anchorable organic sensitizers with indolo[2,3-*b*]quinoxaline moieties: Correlation between structure and DSSC performance, *Sol. Energy*, 2020, **206**, 443–454.

29 R. Su, L. Lyu, M. R. Elmorsy and A. El-Shafei, Structural studies and photovoltaic investigation of indolo[2,3:*B*] quinoxaline-based sensitizers/co-sensitizers achieving highly efficient DSSCs, *New J. Chem.*, 2020, **44**, 2797–2812.

30 (*a*) N. X. Hu, S. Xie, Z. Popovic, B. Ong, A. M. Hor and S. Wang, 5,11-Dihydro-5,11-di-1-naphthylindolo[3,2-*b*]carbazole: Atropisomerism in a novel hole-transport molecule for organic light-emitting diodes, *J. Am. Chem. Soc.*, 1999, **121**, 5097–5098; (*b*) S. Wakim, J. Bouchard, M. Simard, N. Drolet, Y. Tao and M. Leclerc, Organic microelectronics: Design, synthesis, and characterization of 6,12-dimethylindolo[3,2-*b*]carbazoles, *Chem. Mater.*, 2004, **16**, 4386–4388; (*c*) Y. Li, Y. Wu, S. Gardner and B. S. Ong, Novel peripherally substituted indolo[3,2-*b*]carbazoles for high-mobility organic thin-film transistors, *Adv. Mater.*, 2005, **17**, 849–853; (*d*) Y. Wu, Y. Li, S. Gardner and B. S. Ong, Indolo[3,2-*b*]-carbazole-based thin-film transistors with high mobility and stability, *J. Am. Chem. Soc.*, 2005, **127**, 614–618; (*e*) P. T. Boudreault, S. Wakim, N. Blouin, M. Simard, C. Tessier, Y. Tao, M. Leclerc and V. La, Synthesis, characterization, and application of indolo[3,2-b]carbazole semiconductors, *J. Am. Chem. Soc.*, 2007, **129**, 9125–9136.

31 For the synthesis of indolocarbazole see: (*a*) B. Robinson, The Fischer indolisation of cyclohexane-1,4-dione bisphenylhydrazone, *J. Chem. Soc.*, 1963, 3097–3099; (*b*) J. I. G. Cadogan, M. Carmeron-Wood, R. K. Makie and R. I. J. Searle, The reactivity of organophosphorus compounds. Part XIX. Reduction of nitro-compounds by triethyl phosphite: A convenient new route to carbazoles, indoles, indazoles, triazoles, and related compounds, *J. Chem. Soc.*, 1965, 4831.

32 X. H. Zhang, Z. S. Wang, Y. Cui, N. Koumura, A. Furube and K. Hara, Organic sensitizers based on hexylthiophene-functionalized indolo[3, 2-b]carbazole for efficient dye-sensitized solar cells, *J. Phys. Chem. C*, 2009, **113**, 13409–13415.

33 S. Cai, G. Tian, X. Li, J. Su and H. Tian, Efficient and stable DSSC sensitizers based on substituted dihydroindolo[2,3-*b*]carbazole donors with high molar extinction coefficients, *J. Mater. Chem. A*, 2013, **1**, 11295–11305.

34 Y. Wu and W. Zhu, Organic sensitizers from D–π–A to D–A–π–A: Effect of the internal electron-withdrawing units on molecular absorption, energy levels and photovoltaic performances, *Chem. Soc. Rev.*, 2013, **42**, 2039–2058.

35 S. Cai, X. Hu, G. Tian, H. Zhou, W. Chen, J. Huang, X. Li and J. Su, Photo-stable substituted dihydroindolo[2,3-*b*]carbazole-based organic dyes: Tuning the photovoltaic properties by optimizing the π structure for panchromatic DSSCs, *Tetrahedron*, 2014, **70**, 8122–8128.

36 X. Qian, L. Shao, H. Li, R. Yan, X. Wang and L. Hou, Indolo[3,2-*b*]carbazole-based multi-donor–π–acceptor type organic dyes for highly efficient dye-sensitized solar cells, *J. Power Sources*, 2016, **319**, 39–47.

37 Z. Xiao, Y. Di, Z. Tan, X. Cheng, B. Chen and J. Feng, Efficient organic dyes based on perpendicular 6,12-diphenyl substituted indolo[3,2-*b*] carbazole donor, *Photochem. Photobiol. Sci.*, 2016, **15**, 1514–1523.

38 Z. Xiao, B. Chen, Y. Di, H. Wang, X. Cheng and J. Feng, Effect of substitution position on photoelectronic properties of indolo[3,2-*b*]carbazole-based metal-free organic dyes, *Sol. Energy*, 2018, **173**, 825–833.

39 J. Y. Su, C. Y. Lo, C. H. Tsai, C. H. Chen, S. H. Chou, S. H. Liu, P. T. Chou and K. T. Wong, Indolo[2,3-*b*]carbazole synthesized from a double-intramolecular Buchwald–Hartwig reaction: Its application for a dianchor DSSC organic dye, *Org. Lett.*, 2014, **16**, 3176–3179.

40 H. Zhang, Z. E. Chen, J. Hu and Y. Hong, Novel metal-free organic dyes containing linear planar 11,12-dihydroindolo-[2,3-a]carbazole donor for dye-sensitized solar cells: Effects of π spacer and alkyl chain, *Dyes Pigm.*, 2019, **164**, 213–221.

41 C. Luo, W. Bi, S. Deng, J. Zhang, S. Chen, B. Li, Q. Liu, H. Peng and J. Chu, Indolo[3,2,1-*jk*] carbazole derivatives-sensitized solar cells: Effect of π-bridges on the performance of cells, *J. Phys. Chem. C*, 2014, **118**, 14211–14217.

42 W. Cao, M. Fang, Z. Chai, H. Xu, T. Duan, Z. Li, X. Chen, J. Qin and H. Han, New D–π–A organic dyes containing a *tert*-butyl-capped indolo[3,2,1-*jk*]carbazole donor with bithiophene unit as π-linker for dye-sensitized solar cells, *RSC Adv.*, 2015, **5**, 32967–32975.

43 X. C. Li, C. Y. Wang, W. Y. Lai and W. Huang, Triazatruxene-based materials for organic electronics and optoelectronics, *J. Mater. Chem. C*, 2016, **4**, 10574–10587 and references cited therein.

44 For the synthesis of triazatruxene see: (*a*) J. Bergman and N. Eklund, Synthesis of 2,2′-biindolyls by coupling reactions, *Tetrahedron*, 1980, **36**, 1439–1443; (*b*) J. Bergman and N. Eklund, Synthesis and studies of tris-indolobenzenes and related compounds, *Tetrahedron*, 1980, **36**, 1445–1450; (*c*) M. A. Eissenstat, M. R. Bell, T. E. D'Ambra, E. J. Alexander, S. J. Daum, J. H. Ackerman, M. D. Gruett, V. Kumar, K. G. Estep, E. M. Olefirowicz, J. R. Wetzel, M. D. Alexander, J. D. Weaver, D. A. Haycock, D. A. Luttinger, F. M. Casiano, S. M. Chippari, J. E. Kuster, J. I. Stevenson and S. J. Ward, Aminoalkylindoles: Structure–activity relationships of novel cannabinoid mimetics, *J. Med. Chem.*, 1995, **38**, 3094–3105.

45 X. Qian, Y. Z. Zhu, J. Song, X. P. Gao and J. Y. Zheng, New donor-π-acceptor type triazatruxene derivatives for highly efficient dye-sensitized solar cells, *Org. Lett.*, 2013, **15**, 6034–6037.

46 X. Qian, L. Lu, Y. Z. Zhu, H. H. Gao and J. Y. Zheng, Triazatruxene-based organic dyes containing a rhodanine-3-acetic acid acceptor for dye-sensitized solar cells, *Dyes Pigm.*, 2015, **113**, 737–742.

47 B. Pan, Y. Z. Zhu, D. Ye, F. Li, Y. F. Guo and J. Y. Zheng, Effects of ethynyl unit and electron acceptors on the performance of triazatruxene-based dye-sensitized solar cells, *New J. Chem.*, 2018, **42**, 4133–4141.

48 X. Qian, R. Yan, L. Shao, H. Li, X. Wang and L. Hou, Triindole-modified push–pull type porphyrin dyes for dye-sensitized solar cells, *Dyes Pigm.*, 2016, **134**, 434–441.

49 P. Qin, P. Sanghyun, M. I. Dar, K. Rakstys, H. ElBatal, S. A. Al-Muhtaseb, C. Ludwig and M. K. Nazeeruddin, Weakly conjugated hybrid zinc porphyrin sensitizers for solid-state dye-sensitized solar cells, *Adv. Funct. Mater.*, 2016, **26**, 5550–5559.

50 L. Zhang, X. Yang, W. Wang, G. G. Gurzadyan, J. Li, X. Li, J. An, Z. Yu, H. Wang, B. Cai, A. Hagfeldt and L. Sun, 13.6% Efficient organic dye-sensitized solar cells by minimizing energy losses of the excited state, *ACS Energy Lett.*, 2019, **4**, 943–951.

51 L. Zhang, X. Yang, B. Cai, H. Wang, Z. Yu and L. Sun, Triazatruxene-based sensitizers for highly efficient solid-state dye-sensitized solar cells, *Sol. Energy*, 2020, **212**, 1–5.

52 L. Zhang, X. Yang, S. Li, Z. Yu, A. Hagfeldt and L. Sun, Electron-withdrawing anchor group of sensitizer for dye-sensitized solar cells, cyanoacrylic acid, or benzoic acid?, *Sol. RRL*, 2020, **4**, 1900436.

53 S. Li, X. Yang, L. Zhang, J. An, B. Cai and X. Wang, Effect of fluorine substituents on benzothiadiazole-based D–π–A′–π–A photosensitizers for dye-sensitized solar cells, *RSC Adv.*, 2020, **10**, 9203–9209.

54 Z. Yao, X. Liao, Y. Guo, H. Zhao, Y. Guo, F. Zhang, L. Zhang, Z. Zhu, L. Kloo, W. Ma, Y. Chen and L. Sun, Exploring overall photoelectric applications by organic materials containing symmetric donor isomers, *Chem. Mater.*, 2019, **31**, 8810–8819.

55 For the synthesis of indeno[1,2-*b*]indole see: D. W. Brown, M. F. Mahon, A. Ninan, M. Sainsbury and H. G. Shertzer, The Fischer indolisation reaction and the synthesis of dihydroindenoindoles, *Tetrahedron*, 1993, **49**, 8919–8932.

56 X. Qian, R. Yan, C. Xu, L. Shao, H. Li and L. Hou, New efficient organic dyes employing indeno[1,2-*b*]indole as the donor moiety for dye-sensitized solar cells, *J. Power Sources*, 2016, **332**, 103–110.

57 X. Qian, R. Yan, Y. Hang, Y. Lv, L. Zheng, C. Xu and L. Hou, Indeno[1,2-*b*]indole-based organic dyes with different acceptor groups for dye-sensitized solar cells, *Dye. Pigment.*, 2017, **139**, 274–282.

58 R. Yan, X. Qian, Y. Jiang, Y. He, Y. Hang and L. Hou, Ethynylene-linked planar rigid organic dyes based on indeno[1,2-*b*]indole for efficient dye-sensitized solar cells, *Dyes Pigm.*, 2017, **141**, 93–102.

59 P. P. Dai, Y. Z. Zhu, Q. L. Liu, Y. Q. Yan and J. Y. Zheng, Novel indeno[1,2-*b*]indole-spirofluorene donor block for efficient sensitizers in dye-sensitized solar cells, *Dyes Pigm.*, 2020, **175**, 108099.

60 P. P. Dai, J. Han, Y. Z. Zhu, Y. Q. Yan and J. Y. Zheng, Orientation-dependent effects of indeno[1,2-*b*]indole-spirofluorene donor on photovoltaic performance of D–π–A and D–D–π–A sensitizers, *J. Power Sources*, 2021, **481**, 228901.

61 X. Zhou, J. Lu, H. Huang, Y. Yun, Z. Li and F. You, Dyes and pigments thieno[3,2-*b*]indole (TI) bridged A–π–D–π–A small molecules: Synthesis, characterizations and organic solar cell applications, *Dyes Pigm.*, 2019, **160**, 16–24.

62 X. Zhang, Y. Cui, R. Katoh, N. Koumura and K. Hara, Organic dyes containing thieno[3,2-*b*]indole donor for efficient dye-sensitized solar cells, *J. Phys. Chem. C*, 2010, **114**, 18283–18290.

63 N. Koumura, Z. S. Wang, S. Mori, M. Miyashita, E. Suzuki and K. Hara, Alkyl-functionalized organic dyes for efficient molecular photovoltaics, *J. Am. Chem. Soc.*, 2006, **128**, 14256–14257.

64 Y. K. Eom, S. H. Kang, I. T. Choi, Y. Yoo, J. Kim and H. K. Kim, Significant light absorption enhancement by a single heterocyclic unit change in the π-bridge moiety from thieno[3,2-*b*]benzothiophene to thieno[3,2-*b*]indole for high performance dye-sensitized and tandem solar cells, *J. Mater. Chem. A*, 2017, **5**, 2297–2308.

65 J. M. Ji, H. Zhou, Y. K. Eom, C. H. Kim and H. K. Kim, 14.2% efficiency dye-sensitized solar cells by co-sensitizing novel thieno[3,2-*b*]indole-based organic dyes with a promising porphyrin sensitizer, *Adv. Energy Mater.*, 2020, **10**, 2000124.

66 J. M. Ji, S. H. Kim, H. Zhou, C. H. Kim and H. K. Kim, D–π–A-structured porphyrins with extended auxiliary π-spacers for highly efficient dye-sensitized solar cells, *ACS Appl. Mater. Interfaces*, 2019, **11**, 24067–24077.

67 S. H. Kang, S. Y. Jung, Y. W. Kim, Y. K. Eom and H. K. Kim, Exploratory synthesis and photovoltaic performance comparison of D–π–A structured Zn-porphyrins for dye-sensitized solar cells, *Dye. Pigment.*, 2018, **149**, 341–347.

68 R. A. Irgashev, A. A. Karmatsky, S. A. Kozyukhin, V. K. Ivanov, A. Sadovnikov, V. V. Kozik, V. A. Grinberg, V. V. Emets, G. L. Rusinov and V. N. Charushin, A facile and convenient synthesis and photovoltaic characterization of novel thieno[2,3-b]indole dyes for dye-sensitized solar cells, *Synth. Met.*, 2015, **199**, 152–158.

69 R. A. Irgashev, A. A. Karmatsky, G. A. Kim, A. A. Sadovnikov, V. V. Emets, V. A. Grinberg, V. K. Ivanov, S. A. Kozyukhin, G. L. Rusinov and V. N. Charushin, Novel push-pull thieno[2,3-*b*]indole-based dyes for efficient dye-sensitized solar cells (DSSCs), *ARKIVOC*, 2017, 34–50.

70 For the synthesis of indolo[3,2-*b*]indole see: (*a*) S. A. Samsoniya and M. V. Trapaidze, The chemistry of indoloindoles, *Russ. Chem. Rev.*, 2007, **76**, 313 and references cited therein; (*b*) A. N. Grinev and S. Y. Ryabova, New method for the synthesis of indolo [3,2-*b*] indole derivatives, *Chem. Heterocycl. Compd.*, 1982, **18**, 153; (*c*) P. Kaszynski and D. A. Dougherty, Synthesis and properties of diethyl 5,10-dihetera-5,10-dihydroindeno[2,1-*a*]indene-2,7-dicarboxylates, *J. Org. Chem.*, 1993, **58**, 5209; (*d*) L. Qiu, C. Yu, N. Zhao, W. Chen, Y. Guo, X. Wan, R. Yang and Y. Liu, An expedient synthesis of fused heteroacenes bearing a pyrrolo[3,2-*b*]pyrrole core, *Chem. Commun.*, 2012, **48**, 12225–12227; (*e*) L. Qiu, X. Wang, N. Zhao, S. Xu, Z. An, X. Zhuang, Z. Lan, L. Wen and X. Wan, Reductive ring closure methodology toward heteroacenes bearing a dihydropyrrolo[3,2-*B*]pyrrole core: Scope and limitation, *J. Org. Chem.*, 2014, **79**, 11339–11348; (*f*) M. A. Truong and K. Nakano, Synthesis of benzofuro- and indolo[3,2-*b*]indoles *via* palladium-catalyzed double *N*-arylation and their physical properties, *J. Org. Chem.*, 2015, **80**, 11566–11572; (*g*) H. E. Ho, K. Oniwa, Y. Yamamoto and T. Jin, N-Methyl transfer induced copper-mediated oxidative

diamination of alkynes, *Org. Lett.*, 2016, **18**, 2487–2490; (*h*) L. H. Leijendekker, J. Weweler, T. M. Leuther and J. Streuff, Catalytic reductive synthesis and direct derivatization of unprotected aminoindoles, aminopyrroles, and iminoindolines, *Angew. Chem., Int. Ed.*, 2017, **56**, 6103–6106.

71 (*a*) M. M. Murray, D. A. Kaisaki, W. Chang, D. A. Dougherty and P. Kaszynski, Prototypes for the polaronic ferromagnet. Synthesis and characterization of high-spin organic polymers, *J. Am. Chem. Soc.*, 1994, **116**, 8152–8161; (*b*) J. Sim, K. Do, K. Song, A. Sharma, S. Biswas, G. D. Sharma and J. Ko, D–A–D–A–D push pull organic small molecules based on 5,10-dihydroindolo[3,2-*b*]indole (DINI) central core donor for solution processed bulk heterojunction solar cells, *Org. Electron.*, 2016, **30**, 122–130; (*c*) I. Cho, S. K. Park, B. Kang, J. W. Chung, J. H. Kim, K. Cho and S. Y. Park, Design, synthesis, and versatile processing of indolo[3,2-*b*]indole-based π-conjugated molecules for high-performance organic field-effect transistors, *Adv. Funct. Mater.*, 2016, **26**, 2966–2973; (*d*) Y. Y. Lai, J. M. Yeh, C. E. Tsai and Y. J. Cheng, Synthesis, molecular and photovoltaic properties of an indolo[3,2-*b*]indole-based acceptor–donor–acceptor small molecule, *Eur. J. Org. Chem.*, 2013, 5076–5084.

72 N. Ruangsupapichat, M. Ruamyart, P. Kanchanarugee, C. Boonthum, N. Prachumrak, T. Sudyoadsuk and V. Promarak, Toward rational design of metal-free organic dyes based on indolo[3,2-*b*]indole structure for dye-sensitized solar cells, *Dyes Pigm.*, 2018, **151**, 149–156.

73 C. Ruamyart, P. Chasing, T. Sudyoadsuk, V. Promarak and N. Ruangsupapichat, Double anchor indolo[3,2-*b*]indole-derived metal-free dyes with extra electron donors as efficient sensitizers for dye-sensitized solar cells, *New J. Chem.*, 2021, **45**, 7542–7554.

74 P. V. Santhini, V. Jayadev, S. C. Pradhan, S. Lingamoorthy, P. R. Nitha, M. V. Chaithanya, R. K. Mishra, K. N. Narayanan Unni, J. John and S. Soman, Indolo[3,2-*b*]indole donor-based D–π–A dyes for DSCs: Investigating the role of π-spacers towards recombination, *New J. Chem.*, 2019, **43**, 862–873.

75 (*a*) P. V. Santhini, S. A. Babu, A. Krishnan, R. E. Suresh and J. John, Heteroannulation of 3-nitroindoles and 3-nitrobenzo[*b*]thiophenes: A multicomponent approach toward pyrrole-fused heterocycles, *Org. Lett.*, 2017, **19**, 2458–2461; (*b*) P. V. Santhini, R. Akhil Krishnan, S. A. Babu, B. S. Simethy, G. Das, V. K. Praveen, S. Varughese and J. John, One-pot MCR-oxidation approach toward indole-fused heteroacenes, *J. Org. Chem.*, 2017, **82**, 10537–10548.

76 J. Wang, S. Liu, K. Chang, Q. Liao, S. Li, H. Han, Q. Li and Z. Li, Synergy effect of electronic characteristics and spatial configurations of electron donors on photovoltaic performance of organic dyes, *J. Mater. Chem. C*, 2020, **8**, 14453–14461.

77 For the synthesis of benzothieno[3,2-*b*]indole see: (*a*) T. Sugahara, K. Murakami, H. Yorimitsu and A. Osuka, Palladium-catalyzed amination of aryl sulfides with anilines, *Angew. Chem., Int. Ed.*, 2014, **53**, 9329–9333; (*b*) Y. Huang, D. Wu, J. Huang, Q. Guo, J. Li and J. You, Use of the Wilkinson catalyst for the *ortho*-C–H heteroarylation of aromatic amines: Facile access to highly extended π-conjugated heteroacenes for organic semiconductors, *Angew. Chem., Int. Ed.*, 2014, **53**, 12158–12162; (*c*) N. Kamimoto, D. Schollmeyer, K. Mitsudo, S. Suga and S. R. Waldvogel, Palladium-catalyzed domino C–H/N–H functionalization: An efficient approach to nitrogen-bridged heteroacenes, *Chem. – Eur. J.*, 2015, **21**, 8257–8261; (*d*) H. Huang, P. Dang, L. Wu, Y. Liang and J. Liu, Copper-catalyzed synthesis of benzo[*b*]thiophene-fused imidazopyridines *via* the cleavage of C–H bond and C–X bond, *Tetrahedron Lett.*, 2016, **57**, 574–577; (*e*) X. Zhao, Q. Li, J. Xu, D. Wang, D. Zhang-Negrerie and Y. Du, Cascade synthesis of benzothieno[3,2-*b*]indoles under oxidative conditions mediated by CuBr and *tert*-butyl hydroperoxide, *Org. Lett.*, 2018, **20**, 5933–5937; (*f*) X. H. Shan, B. Yang, J. P. Qu and Y. B. Kang, $CuSO_4$-Catalyzed dual annulation to synthesize O, S or N-containing tetracyclic heteroacenes, *Chem. Commun.*, 2020, **56**, 4063–4066.

78 (*a*) Q. Ji, J. Gao, J. Wang, C. Yang, X. Hui, X. Yan, X. Wu, Y. Xie and M. W. Wang, Benzothieno[3,2-*b*]indole derivatives as potent selective estrogen receptor modulators, *Bioorg. Med. Chem. Lett.*, 2005, **15**, 2891–2893; (*b*) S. A. Al-Trawneh, M. M. El-Abadelah, J. A. Zahra, S. A. Al-Taweel, F. Zani, M. Incerti, A. Cavazzoni and P. Vicini, Synthesis and biological evaluation of tetracyclic thienopyridones as antibacterial and antitumor agents, *Bioorg. Med. Chem.*, 2011, **19**, 2541–2548; (*c*) M. Ning, C. Zhou, J. Weng, S. Zhang, D. Chen, C. Yang, H. Wang, J. Ren, L. Zhou, C. Jin and M. W. Wang, Biological activities of a novel selective oestrogen receptor modulator derived from raloxifene (Y134), *Br. J. Pharmacol.*, 2007, **150**, 19–28.

79 R. K. Konidena, K. H. Lee, J. Y. Lee and W. P. Hong, A new benzothienoindole-based bipolar host material for efficient green phosphorescent organic light-emitting diodes with extremely small efficiency roll-off, *Org. Electron. Phys., Mater. Appl.*, 2019, **70**, 211–218.

80 P. R. Nitha, V. Jayadev, S. C. Pradhan, V. Divya, C. H. Suresh, J. John, S. Soman and A. Ajayaghosh, Regulating back electron transfer through donor and π-spacer alterations in benzothieno[3,2-*b*]indole-based dye-sensitized solar cells, *Chem. – Asian J.*, 2020, **15**, 3503–3512.

81 For the synthesis of tetraindole see: (*a*) H. Hiyoshi, T. Sonoda and S. Mataka, Synthesis of cyclic novel symmetric cyclic indole-tetramers, *Heterocycles*, 2006, **68**, 763–769; (*b*) F. Wang, X. C. Li, W. Y. Lai, Y. Chen, W. Huang and F. Wudl, Synthesis and characterization of symmetric cyclooctatetraindoles: Exploring the potential as electron-rich skeletons with extended π-systems, *Org. Lett.*, 2014, **16**, 2942–2945.

82 X. Qian, H. H. Gao, Y. Z. Zhu, B. Pan and J. Y. Zheng, Tetraindole-based saddle-shaped organic dyes for efficient dye-sensitized solar cells, *Dye. Pigment.*, 2015, **121**, 152–158.

83 H. Cheng, Y. Wu, J. Su, Z. Wang, R. P. Ghimire, M. Liang, Z. Sun and S. Xue, Organic dyes containing indolodithienopyrrole unit for dye-sensitized solar cells, *Dyes Pigm.*, 2018, **149**, 16–24.

84 R. Bisht, V. Sudhakar, M. Fairoos, M. Kavungathodi, N. Karjule and J. Nithyanandhan, Fused fluorenylindolenine donor based unsymmetrical squaraine dyes for dye-sensitized solar cells, *ACS Appl. Mater. Interfaces*, 2018, **10**, 26335–26347.

85 S. Ramasamy, ScienceDirect organic photosensitizers containing fused indole- imidazole ancillary acceptor with triphenylamine donor moieties for efficient dye-sensitized solar cells, *Int. J. Hydrogen Energy*, 2021, **46**, 3475–3483.